Am J Physiol Cell Physiol 322: C674–C687, 2022.
First published February 23, 2022; doi:10.1152/ajpcell.00019.2022

american physiological society

AMERICAN JOURNAL OF PHYSIOLOGY
CELL PHYSIOLOGY

REVIEW

Deciphering the Role of Proteoglycans and Glycosaminoglycans in Health and Disease

Methods for isolating and analyzing physiological hyaluronan: a review

Felipe Rivas,[1] Dorothea Erxleben,[1] Ian Smith,[1] Elaheh Rahbar,[1] Paul L. DeAngelis,[2] Mary K. Cowman,[3,4] and Adam R. Hall[1,5]

[1]*Virginia Tech-Wake Forest University School of Biomedical Engineering and Sciences, Wake Forest School of Medicine, Winston-Salem, North Carolina;* [2]*Department of Biochemistry and Molecular Biology, University of Oklahoma Health Sciences Center, Oklahoma City, Oklahoma;* [3]*Department of Biomedical Engineering, New York University Tandon School of Engineering, New York, New York;* [4]*Department of Orthopedic Surgery, New York University Grossman School of Medicine, New York, New York; and* [5]*Comprehensive Cancer Center, Wake Forest School of Medicine, Winston-Salem, North Carolina*

Abstract

The carbohydrate hyaluronan (or hyaluronic acid, HA) is found in all human tissues and biofluids where it has wide-ranging functions in health and disease that are dictated by both its abundance and size. Consequently, hyaluronan evaluation in physiological samples has significant translational potential. Although the analytical tools and techniques for probing other biomolecules such as proteins and nucleic acids have become standard approaches in biochemistry, those available for investigating hyaluronan are less well established. In this review, we survey methods related to the assessment of native hyaluronan in biological specimens, including protocols for separating it from biological matrices and technologies for determining its concentration and molecular weight.

extraction; hyaluronan; quantification; size distribution; translational biomarkers

INTRODUCTION

Hyaluronan (or hyaluronic acid; HA) is a linear glycosaminoglycan (GAG) composed of the alternating disaccharide repeat structure [-4-D-glucuronic acid-β1-3-*N*-acetyl D-glucosamine-β1-]$_n$ that was first reported nearly a century ago by Meyer and Palmer (1), who derived its name from the biological matrix from which it was sourced ("hyaloid," for vitreous humor) and the major chemical constituent it contained (uronic acid). Structurally, HA does not exhibit the substituent sulfation that is typical of other GAGs (2–4), resulting in a consistent chemical configuration and negative electrostatic charge at physiological pH. As a semiflexible anionic polymer, HA forms a hydrated entropic coil in solution that can produce nonlinear viscoelastic properties through coil-coil interactions (5). In free solution, this behavior is driven by physical crowding, dictated largely (6) by HA concentration and polymer size (i.e., larger molecules occupy more entropic volume and promote domain overlap). However, in physiological systems, the activity of binding entities is another major contributing factor. Although the only natural covalent alteration known to impact HA is the attachment of the inter-α-inhibitor heavy chain (HC) domain by the catalytic activity of the tumor necrosis factor-inducible-gene 6 (TSG-6) enzyme (7), a variety of noncovalent interactions with proteoglycans and other proteins (8) are also known to occur, facilitating the variation of intermolecular interfaces and consequently of the local physicochemical environment in vivo.

As a component of diverse mammalian tissues and biofluids (9, 10) [as well as other, nonmammalian systems (11–13)], HA exists in various quantities (14) and is generally polydisperse, covering a broad range (9) of molecular weight (MW) from ~10^5 to 10^7 Da (~250–25,000 disaccharide units). In its ubiquity, HA is known to play critical roles in diverse biological functions like extracellular matrix structure (9), hydration and turgidity maintenance of tissue (9), regulation of innate immunity (15), tissue regeneration and repair (16), and the protection and lubrication of joints (17), each of which can be impacted by its particular size distribution (i.e., low vs. high MW). This diversity also makes clear the corresponding importance of HA to pathological processes, and its abundance and/or size distribution have indeed been identified as a major factor in diseases that include liver fibrosis (18, 19), amyotrophic lateral sclerosis (20), multiple sclerosis (21), acute kidney injury (22), myocardial ischemia (23), osteoarthritis (24–26), and various forms of cancer (27–31). The importance of HA as a potential bioindicator necessitates robust technologies for elucidating its complex interactions with the physiological environment and subsequently for

Correspondence: A. R. Hall (arhall@wakehealth.edu).
Submitted 17 January 2022 / Revised 22 February 2022 / Accepted 22 February 2022

assessing it in clinical specimens toward patient diagnosis and prognosis. Here, we will review the major approaches relevant to this goal, including both the purification of HA from diverse biological specimens and the determination of its properties.

HA ISOLATION AND EXTRACTION METHODS

HA analytical techniques typically require pure samples, either due to intrinsic nonselectivity or potential interference from background contaminants. For this reason, pretreatment of native biospecimens is critical. Broadly, the approaches for HA separation from its physiological matrix can be classified in two groups: isolation, or the removal of nontarget components to leave pure HA behind, and extraction, or the specific retrieval of HA from a complex milieu based on its physical or chemical properties.

Toward isolation, a variety of chemical and biochemical techniques have been adapted to HA since the earliest reports of its retrieval. These approaches necessitate some protocol differences based on the properties of the starting material; for example, bone (32) is flash frozen and powdered by milling, blood (33) or conditioned media (34) are centrifuged to remove cells, and egg shell (35, 36) is decalcified by acetic acid or EDTA. However, outside of these pretreatments, a common set of treatments is generally used, either concurrently (37) or more typically in a stepwise manner. First, lipids can be removed by a variety of solvents, including acetone (1, 13, 38–41) or chloroform-methanol (35, 42–44) followed by enzymatic digestion of protein components, often using broad-spectrum proteases such as proteinase K or pronase (40, 42, 45–51). It has been noted (45) that some broad-spectrum proteases can induce HA degradation (likely due to contaminating glycanases, highlighting the utility of process validation with "spiked" HA internal standards) and so a more directed protease (32, 35, 36, 41, 44, 52) may also be selected depending on the specimen type. Finally, nucleic acids are digested by nuclease treatment (33, 47, 53–56) and then all utilized enzymes are commonly inactivated by heat (41, 48, 53), leaving GAGs in solution with the remaining digest and cleavage products. If necessary (dependent on protease selection), the GAGs may be further processed to remove core protein peptide fragments through β-elimination (40, 44) or other chemical treatments (13, 32), but are then generally separated from residual material via chloroform extraction and/or ethanol precipitation (13, 34, 49, 52) or with detergents (35).

Because all GAGs coprecipitate with these recovery strategies, the challenge then becomes removal of off-target species to isolate HA alone. In principle, this could be achieved with selected GAG lyases (57), but in practice, many tend to have cross-reactivity with HA that can result in unintended degradation. To circumvent this, the unsulfated nature of HA has been exploited through strategies designed to specifically remove sulfated GAGs, including chemical fractionation with either cetylpyridinium chloride (58) or ethanol (59) and ion exchange chromatography (39).

Although historically critical to the study of HA, isolation strategies have significant drawbacks. For example, they are limited in their ability to achieve ultrahigh purity HA samples, because non-HA GAGs can display variable sulfation (2, 60), off-target contaminants can be co-segregated with HA (51). In addition, the multiple steps and purifications generally required for the implementation of these approaches can be lossy, reducing HA yield, especially in biological matrices with low relative starting abundance. For these reasons, extraction techniques are more common in modern processes.

Immunoprecipitation (IP) has been used commonly for small-scale affinity purification and isolation of proteins. In the general technique, target-specific antibodies are immobilized on a substrate (e.g., on gel/resin or beads) and used to bind to the protein of interest selectively from a mixture. Once captured, excess material is removed (or, in the case of beads, the substrate is pelleted and washed) and target proteins are eluted to recover the target material, providing high-purity product. The IP concept was first applied to HA extraction by Yuan et al. (46) who substituted antibodies with hyaladherins to achieve selective capture of HA from human breast milk. As a substrate, commercial streptavidin-coated paramagnetic beads were used after conjugation to highly HA-specific versican G1 domains (VG1) via a biotin moiety, enabling fast pelleting under an applied magnetic field. To avoid interference, isolation steps (like those described earlier) were used to remove or degrade macromolecules (lipids, proteins, and nucleic acids) and salts from the raw specimen. However, cleanup requirements were less stringent due to VG1 specificity. Collected HA could subsequently be eluted via heat denaturation of the VG1. This versatile approach (or slight variations of it) has been extended to extract HA from several complex biological specimens including synovial fluid (50, 61), blood, urine, ovarian tissue (62), and mouse brain (56).

Some key challenges remain to be addressed with the existing IP protocol. For example, elution by heat denaturation renders the VG1 permanently inactive, preventing repeat captures and increasing reagent costs. Other approaches like proteinase K degradation have proven viable but have the same difficulty. In addition, the recovery fidelity of HA capture must be more fully validated; due to the nature of diffusion kinetics, low-MW (LMW) HA moves faster through solution than high-MW (HMW) HA and this can allow LMW HA to access binding sites more efficiently, creating potential bias that will persist through downstream analyses. Care must be taken to ensure captured HA is representative of the native distribution.

QUANTITATIVE MEASUREMENT APPROACHES FOR HA

Because HA lacks chemical variation, analytical techniques focus on two main values of critical importance to its biological activity: abundance and MW. In this section, we describe approaches for probing each of these factors in turn.

HA Concentration Determination

Physiological HA experiences a high rate of turnover (9) that is governed by associated metabolic (63, 64) and catabolic (65–67) pathways. In healthy individuals, a homeostatic balance is generally maintained such that

HA concentration tends to be relatively consistent in a given tissue or biofluid (10). However, pathologies that impact either the production or (more often) the clearance of HA can have a significant impact on its abundance in vivo. For this reason, changes in HA concentration have been associated with several disease states in humans, including liver diseases [cirrhosis (68, 69) and fibrosis (70)], osteoarthritis (71, 72), and certain cancers (73, 74), and is currently in clinical use as a urinary biomarker of bladder cancer (75, 76).

There are several options for HA quantification in biospecimens. Although conventional techniques used in biochemistry have been applied, such protocols generally have critical limitations. For example, high-performance liquid chromatography (HPLC) has recently been implemented with ultraviolet detection to probe HA viscosupplements (77), but the potential for interference from background constituents in complex biological specimens reduces specificity and necessitates comparative analyses on the same sample both with and without hyaluronidase treatment to assess HA. As a result, this method has reduced translational capacity. Mass spectrometry has also been applied (78, 79) but its dynamic range has an upper limit of ~10–50 kDa. Consequently, it typically requires complete hydrolysis of the HA, similar to HPLC, thus precluding downstream size analysis. For these reasons, alternative methods for quantification are typically used for HA derived from biospecimens.

Imaging modalities.

A number of imaging techniques have been used for probing HA. For example, histological analysis, through which HA in cell culture or tissues is labeled for direct imaging, has been demonstrated for a wide range of specimens (80–86). Because HA-specific antibodies are not available (HA is a "self" molecule) (87), labeling of HA has been enabled instead by highly specific HA binding proteins, especially the cartilage link protein (88), the aggrecan terminal fragment globular domain 1-interglobular domain-globular domain 2 (G1-IGD-G2 or HA binding protein, HABP) (89), and VG1 (90). Of these, HABP and VG1 have comparably high specificity and affinity, but the cartilage link protein is less efficacious and in modern protocols is generally avoided (and is a common contaminant in HABP isolated from bovine nasal cartilage, for example). Although histological HA assessment is often qualitative, content determination can be performed either fluorometrically (91) or using a secondary radiolabeling technique (81), both of which provide the added benefit of also localizing HA in the tissue. However, among the significant disadvantages of this approach are its inability to deliver direct quantification, instead of assessing HA levels relative to an internal standard or between conditions, and its limitations with viable biological matrices (i.e., biological fluids cannot be assessed). A second imaging modality that has been applied to HA quantification is magnetic resonance imaging (MRI) supplemented with chemical exchange saturation transfer (CEST) (92) wherein proton spins in HA are saturated and exchanged with the bulk water surrounding them, resulting in an enhancement in image contrast. Quantification of HA can be derived subsequently from the integrated CEST signal. Due to the noninvasive nature of MRI, this approach has the major advantage of being applicable to live imaging of tissues (23), especially monitoring the behavior and lifetime of implanted HA-biomaterials (i.e., macroscopic amounts of relatively pure HA). However, a significant drawback is its limited specificity for HA; CEST results in an image enhancement for exchangeable protons in general and so off-target analytes like proteins and other GAGs can contribute to the signal, strongly impacting accurate HA quantitation. In addition, like all imaging modalities, CEST cannot provide HA MW information.

ELISA-like assays.

The most widely used techniques for the determination of HA concentration are extensions of the enzyme-linked immunosorbent assay (ELISA), the antibody-based approach initially developed for quantifying protein antigens (93). As described earlier for histological imaging, ELISA quantification uses HA binding proteins like the cartilage link protein, the HABP portion of aggrecan, and VG1. Two ELISA-like assay formats are typical for HA: sandwich assays (94–99) (Fig. 1*A*) in which sample HA is introduced to a surface-bound binding agent and a second, labeled binding agent is then provided to enable quantification through double binding, or competitive assays (97, 100–104) (Fig. 1*B*) in which labeled binding agent is introduced to surface-bound HA and then its displacement through competition with sample HA is used to determine quantity. Several strategies have been demonstrated for labeling HA binders, including radiolabeling, fluorescence, biotinylation (with subsequent streptavidin labeling), and chemiluminescence. Although both sandwich and competitive ELISA-like assays are common and offer high concentration resolution (typically 25 ng/mL) (105), it has been noted that sandwich assays in particular are biased toward high-molecular weight HA (96, 99, 106) and thus fail to quantify smaller fragments accurately.

AlphaScreen. An emerging alternative approach to HA quantification is an adaptation of the Luminescent Oxygen Channeling Immunoassay (107), conducted commercially for drug discovery under the name AlphaScreen. In the general procedure (Fig. 1*C*), two types of beads are used: donor beads loaded with chromophores that can generate singlet oxygen when excited optically; and acceptor beads loaded with separate chromophores that react with singlet oxygen to chemiluminescence. The reaction is proximity-dependent due to the short lifetime of singlet oxygen and so only occurs efficiently when the two beads are physically separated by no more than ~200 nm.

In the modified assay developed for HA (108), the donor beads are conjugated to short biotinylated HA (50 kDa) through streptavidin coupling and the acceptor beads are bound to HABP, enabling the HA-HABP interaction to keep the beads in close proximity and producing a robust chemiluminescent signal. Introduction of unknown sample HA competes for HABP, releasing the bead complex and reducing the signal in a concentration-dependent manner. Using this approach to quantify HA, AlphaScreen provides similar concentration resolution to ELISA techniques (30 ng/mL) but requires less sample volume (108) (2.5 μL vs. 100 μL) and avoids labor-intensive washing steps of the plate-based methods.

The ELISA-like assays and the AlphaScreen assay are both somewhat tolerant of sample purity due to their respective

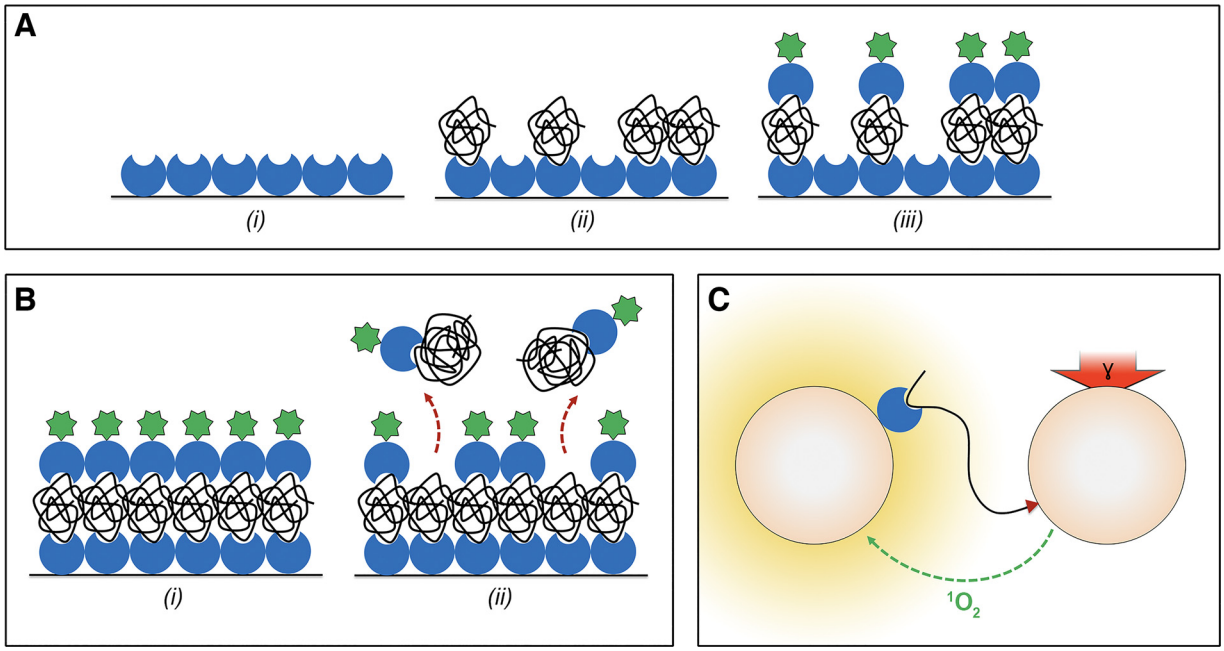

Figure 1. *A*: sandwich enzyme-linked immunosorbent assay (ELISA)-like assay wherein surface-bound hyaluronan (HA) binding proteins *i*) are contacted with specimen HA *ii*) and labeled (green) secondary HA binding proteins are introduced for quantification *iii*). *B*: competitive ELISA-like assay in which surface-bound HA binding proteins preloaded with standard HA and labeled secondary HA binding proteins *i*) are contacted with specimen HA *ii*) that competes for labeled entities and reduces signal. *C*: AlphaScreen construct composed of a donor bead with bound HA (*right*) that creates singlet oxygen upon optical excitement (γ), diffusing to an acceptor bead (*left*) held proximal by a surface-bound HA binding protein thereby producing emission (yellow). Competitive binding with specimen HA will reduce signal as in (*B*).

specificities of binding and so only factors that could impact measurement efficacy need to be managed. For example, HA binding proteins in solution will compete for HA with assay probe proteins and active aggrecanases (109) can cleave HABP and have detrimental effects on HA binding. Therefore, aside from protein degradation, only moderate purification steps are required and should in fact be avoided as possible due to the potential for sample loss that could impact accurate HA quantification. However, a central limitation for each of these techniques is their inability to assess MW as the second major figure of merit for HA. For this, additional techniques are required.

Molecular Weight Determination

HA is naturally polydisperse in all organisms, but the particular MWs present in a given specimen are critical to its behavior. Indeed, a remarkable dichotomy exists in this size-function relationship, with the activity of HMW HA relative to LMW HA (110–116)—or in some cases a narrow distinct MW range relative to other sizes (51, 117)—being contradictory. A critical example of this phenomenon is in inflammation. In its usual HMW conformation in the glycocalyx and extracellular matrix (9), HA acts as a tissue integrity signal and is thus anti-inflammatory in a number of ways (118), including interacting with cell surface receptors to prevent immune cell recognition (119), reducing inflammatory cytokines (120), and inducing STAT5 signaling in regulatory T-cells to promote their maintenance (121). Under inflammatory conditions, however, an abundance of LMW HA (<~500 kDa) is found, likely due to damage and/or degradation. It has been shown that LMW HA is instead proinflammatory in several respects, including upregulating the transcription of inflammatory genes (e.g., TNF-α, IL-1β) (122, 123) and stimulating growth factors (124) and other inflammatory elements (125, 126) in macrophages. Stark contrasts in size-dependent HA functions have also been reported in processes like cell migration/invasion (127–129), angiogenesis (130, 131), and joint lubrication (120), among others. Consequently, determination of MW is critical to the validity of HA as a translational bioindicator of disease.

Viscometry.

Viscometry is a method to analyze and measure bulk HA solution flow that can yield average molecular weight information (132). As HA MW (and/or concentration) increases, increased polymer chain entanglement will increase viscosity and impede the free flow of the liquid in a way that can be measured. Typically, a purified HA solution is either: *1*) flowed through a calibrated tube or capillary with the force of gravity and the speed of transit between two marks is measured; or *2*) positioned between one mobile (rotor) and one stationary (stator) plate or cylinder and the forces for starting or stopping the rotor element is monitored. In both cases, HA MW is determined using the Stokes–Einstein equation and tables based on previous model HA studies using biophysical sedimentation. However, viscometry has several practical challenges, including the requirement for large sample sizes (up to 1 g of HA, depending on chain size and the device) and variability induced by the dependence of viscosity on experimental factors like ionic strength and temperature. Moreover, viscometry can only provide a mean MW rather than distribution. Still, industry often uses the

technique for product quality checks as it is a simple, well-established method to obtain average MW information from HA.

Multi-angle light scattering.

Light scattering (LS), a method to analyze HA MW from the angular distribution and intensity of photons interacting with macromolecules, is a relatively sensitive process that has the advantage of not requiring comparison to a standard. Two modes of LS are practiced: multi-angle light scattering (MALS) (133) and dynamic light scattering (DLS). Typically, the former is used for HA MW analysis (from ~7 kDa to several MDa); the latter is more suited for particle sizing (e.g., cross-linked gels). From a practical standpoint, the required HA sample size for MALS depends on the relative MW of the polymer since larger molecules scatter light more strongly than smaller ones. In the simplest embodiment, a known concentration of purified HA (as contaminants can skew results) is injected into a liquid cell and the MW and polydispersity results are obtained based on the intensity and angular distribution of scattered light. The more angles of scattering data that are used, the better the MW determination; currently, modern detectors simultaneously measure from 3 to 17 angles.

Typically, most modern MALS instruments used a HPLC-size exclusion chromatography (HPLC-SEC) approach as both a separation method and "pre-filter" (dust and contaminant particles can overshadow the target HA) as well as an independent means to assess size distribution. In addition, after the MALS detector, an in-line tandem refractometer is used to measure the concentration of HA; this is especially useful for smaller samples (e.g., precious patient extracts and trials of synthetic products) where the exact concentration is not known. To determine MW, the amount of scattered light and concentration are related through a refractive index increment constant (dn/dc) that is derived empirically by injecting a series of HA solutions of known concentration in a defined buffer solution into the MALS cell sequentially. Many workers in the field use a known buffer such as neutral phosphate buffered saline (0.15 M NaCl) with an established dn/dc value (ranging from 0.153 to 0.167) to avoid unknowns and promote reproducibility. In addition, this buffer is often regarded as compatible with physiological processes. A monodisperse protein standard like bovine serum albumin (66 kDa) is often used to align the outputs of the two detectors, the refractive index, and light scattering cells, as well as calibrate MW and thus validate system performance.

Field flow fractionation (FFF) is also used as a separation method for very high MW [>1–2 MDa HA polymers (134)]; in the MDa range, most existing size exclusion resins are not as useful and can cause some chain shearing, leading to a lower apparent MW value. In a simplistic description of a useful permutation of FFF, the HA sample flows down an open channel similar to chromatographic approaches, but the device simultaneously uses an additional perpendicular fluid flow across a semipermeable membrane along the axis of the channel. Because larger molecules are more affected than the smaller molecules by the cross-flow, HA molecules can be separated according to size and quantified separately. Currently, these devices are more expensive and less numerous than HPLC-SEC setups.

One challenge with MALS approaches is their requirement for significant amounts of HA, dependent on MW and size distribution. By way of example, HA synthesized chemoenzymatically in vitro (135, 136) can achieve a polydispersity index (PDI, or the ratio of the number-average MW to the weight-average MW) of 1.005–1.05, close to a truly monodisperse (PDI = 1.0) polymer. For such quasi-monodisperse HA >500 kDa, ~5–20 μg may be needed for analysis whereas polymers <50 kDa may require 75–100 μg. In physiological HA, the PDI is typically ~1.3–2.0, and since SEC does not allow the majority of HA to be in the MALS detector cell at once (i.e., the wide peak is spread over the elution time), ~2–5 times more sample may be needed. MALS measurements are intrinsically rapid but are limited by the HPLC-SEC or FFF step such that each test will typically take ~15–60 min, and at least duplicate runs should be performed. The absolute MW obtained through MALS is widely recognized as the gold standard, but the accuracy of the size distributions it can deliver is somewhat limited by the separation method resolution.

Gas-phase electrophoretic mobility molecular analysis.

Gas-phase electrophoretic mobility molecular analysis (GEMMA) measures the electrophoretic mobility of single-ionized, spherical molecules and constructs in air to estimate MW. This technique has previously been used to differentiate MWs of globular proteins and viruses (137–139). However, Malm et al. (140) demonstrated that the logarithmic dependence of electrophoretic mobility diameter (EMD) for HA (with the exception of small HA oligomers) can be used to produce a reliable assessment of MW in the range of 30–2,400 kDa, spanning most of its typical physiological range. Like MALS, GEMMA requires a highly purified HA sample as contaminants will skew the results. But in contrast to HPLC-SEC, only a single calibration of analyte electrophoretic mobility is needed rather than routine calibrations, and the resolution of GEMMA is comparable with SEC such that its ability to produce a full MW distribution is limited; it is most effective for comparing distributions of GEMMA spectra between groups (e.g., healthy and pathological tissues).

Measurement time for one spectrum is rapid (5–10 min) and requires as little as 6 pg of total HA, making it an excellent tool for determining the MW of HA from biological specimens with low HA concentrations (141), including tissue samples from small rodents (e.g., mice) and small volume biological fluids (e.g., cerebrospinal fluid and bronchial lavage). However, one intrinsic limitation of the GEMMA approach is the assumption of spherical molecules: variation in instantaneous polymer conformation can produce deviations from this model that may cause measurement inaccuracies. For example, the technique has been shown (140) to underestimate MW for HA molecules > 70 kDa.

Gel electrophoresis.

Gel electrophoresis is a simple and inexpensive method to estimate the MW distribution of unlabeled HA samples ranging in size (142–150) from a few kDa up to at least 6,000 kDa that has been used to analyze HA isolated from numerous tissues and biofluids including skin (49, 151), skeletal muscle (151), heart (151), lung (47, 151), brain (56), small and large intestine (151), mammary gland (54), cervix (152), synovial

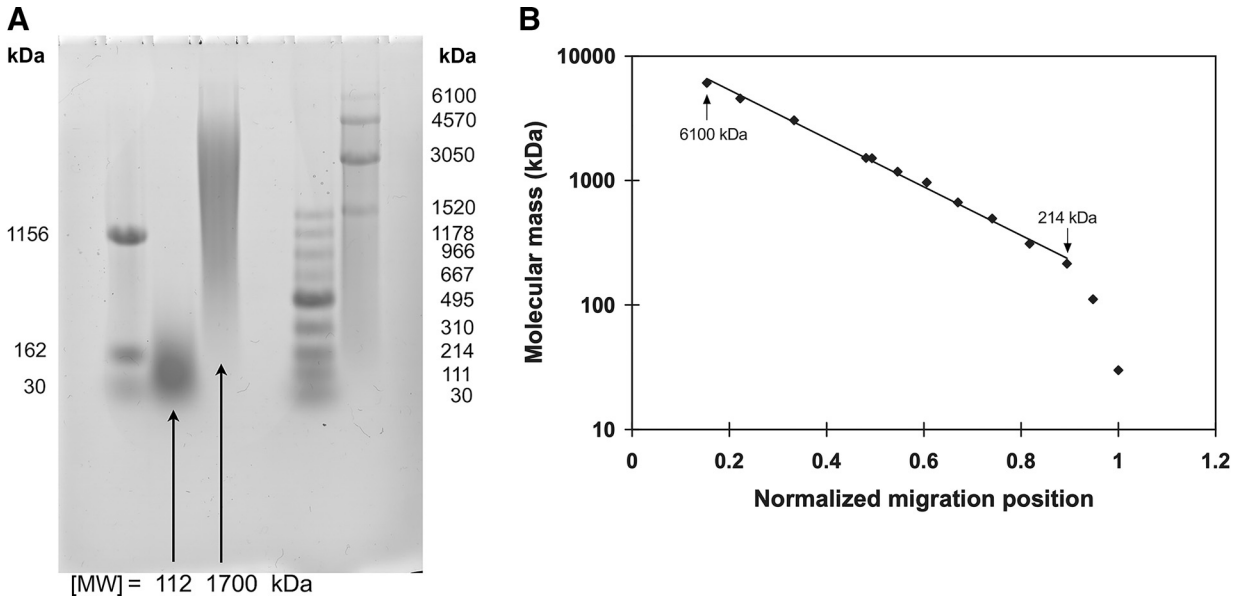

Figure 2. *A*: electrophoresis of hyaluronan (HA) on 0.5% agarose in Tris-acetate-EDTA (TAE) buffer, stained with Stains-All dye. The chemoenzymatically synthesized HA standards appear as sharp bands, but HA isolated from tissue or bacterial sources appears highly polydisperse. The viscosity-average molecular weight (MW) of the two polydisperse samples is indicated. *B*: calibration plot for electrophoretic migration of HA standards. Migration distance for each band was normalized to the migration distance of the smallest HA species. Adapted with permission from Ref. 144. Copyright 2011, Elsevier Inc.

fluid (10, 50, 61, 144), vitreous (144), milk (46), lymph fluid (153), and the conditioned medium of cultured cells (53, 63, 154–162). The charge-to-mass ratio is constant for all HA molecules due to the homogeneous repeating primary structure containing one negatively charged carboxyl group per disaccharide. Thus, like DNA or denatured proteins, migration of HA through a gel matrix under the influence of an applied electric field allows sieving on the basis of size. At the end of the migration time, cationic dyes like Stains-All can be used to immobilize and label HA in the gel (163). Densitometric analysis of the stained pattern can then allow determination of the mean MW and distribution of MWs (polydispersity) of HA in the sample.

Generally, HA greater than ~100 kDa is best size-separated and analyzed on agarose gels (Fig. 2) using total HA mass in the range of 0.1–7 μg, depending on polydispersity and staining method. The applicable MW range depends on agarose concentration and buffer. Concentrations of 0.5%–2% agarose are used most commonly, typically with Tris-borate-EDTA (TBE) or Tris-acetate-EDTA (TAE) (150) as buffer. HA from ~5–100 kDa can be size separated and analyzed best by polyacrylamide gel electrophoresis (Fig. 3)

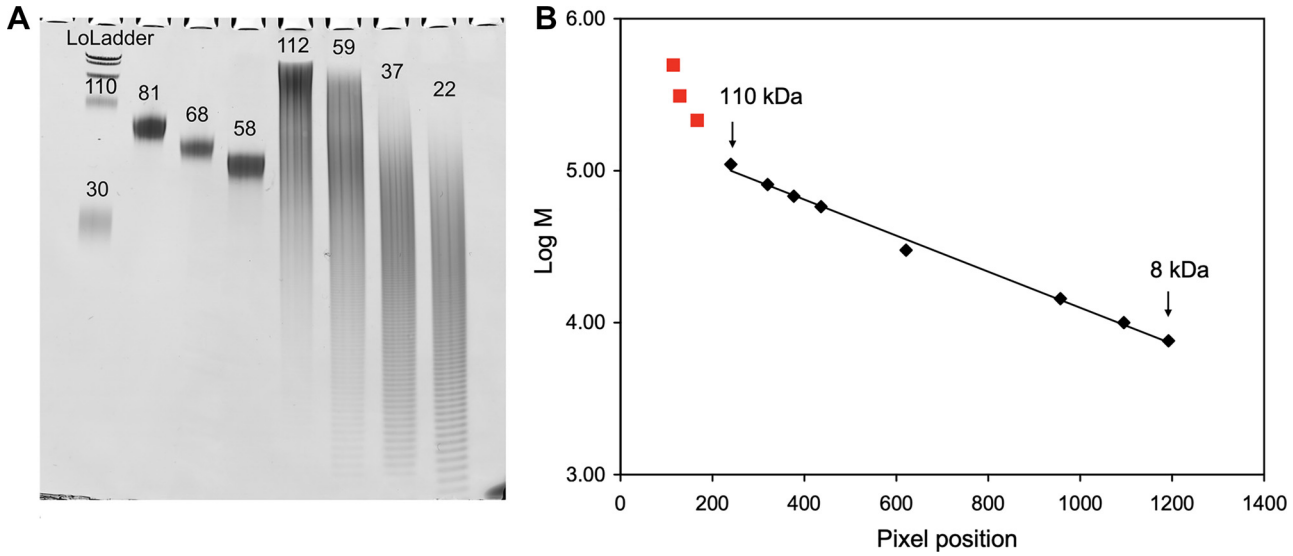

Figure 3. *A*: electrophoresis of hyaluronan (HA) on a 4%–20% polyacrylamide gradient gel in Tris-borate-EDTA (TBE) buffer, with detection by Stains-All dye. Chemoenzymatically synthesized HA standards appear as discrete bands, but HA samples obtained by controlled degradation of high-molecular weight (HMW) HA appeared highly polydisperse. The viscosity-average molecular weight (MW) values of the polydisperse samples are indicated. *B*: calibration plot for electrophoretic migration of HA standards. Adapted with permission from Ref. 143. Copyright 2011, Elsevier Inc.

using total HA mass of ~0.5–1.0 μg. Simple gels containing a constant acrylamide concentration (e.g., 10%) can be used, but commercially available gradient gels (e.g., 4%–20% acrylamide) in TBE buffer can yield excellent separation. All HA larger than ~100 kDa moves slowly, but the resulting sharp bands can be analyzed to quantify as little as 0.1 μg HA by densitometric analysis. At the other extreme, HA oligosaccharides smaller than ~11 disaccharides (4.4 kDa) cannot be detected quantitatively by dyes (142) (possibly due to poor immobilization in the gel), but can be analyzed by the fluorophore-assisted carbohydrate electrophoresis (FACE) method (78, 147, 164–170), which uses reducing-end labeling of the oligosaccharides with a fluorescent dye before electrophoresis so that no additional staining and de-staining procedure is needed.

HA standards must be co-electrophoresed in the same gel used for unknown samples to create a standard curve for size analysis. Chemoenzymatically synthesized quasi-monodisperse HAs (135, 136) are good for this purpose. Sample purification is also a consideration but HA does not need to be highly pure to be analyzed by gel electrophoresis, especially if specific detection is used. However, it must be free of strongly bound proteins like aggrecan or HC, which can cause an electrophoretic mobility shift (149), and non-HA anionic contaminants that can be stained by nonspecific dyes like Stains-All or Alcian Blue +/− silver staining. An HA-specific hyaluronidase from *Streptomyces* [but not testicular hyaluronidase as it can also digest chondroitins (171)]) can be used to confirm the identity of bands (46). Notably, a detailed protocol for agarose gel electrophoresis of HA has been published previously (150). Instructions and spreadsheets for analysis of densitometric scans, and calculation of weight-average and number-average molecular masses have been included as Supplemental Material files in a published method (148).

Nanopore analysis.

Nanopore analysis is an emergent single-molecule approach in which a thin membrane containing an individual, nanometer-scale aperture is positioned between two reservoirs of electrolyte solution and an applied voltage is used to transport molecules introduced to one reservoir through the pore electrophoretically (Fig. 4*A*). The translocation creates a temporary reduction in the measured ionic current passing through the pore (Fig. 4*A*, *insets*), the characteristics of which can convey properties of the passing molecule: for example, signal duration indicates molecular length and signal amplitude (blockage depth) corresponds to molecular diameter. Currently, there are two classes of nanopore platforms: biological nanopores (173–175), composed of a

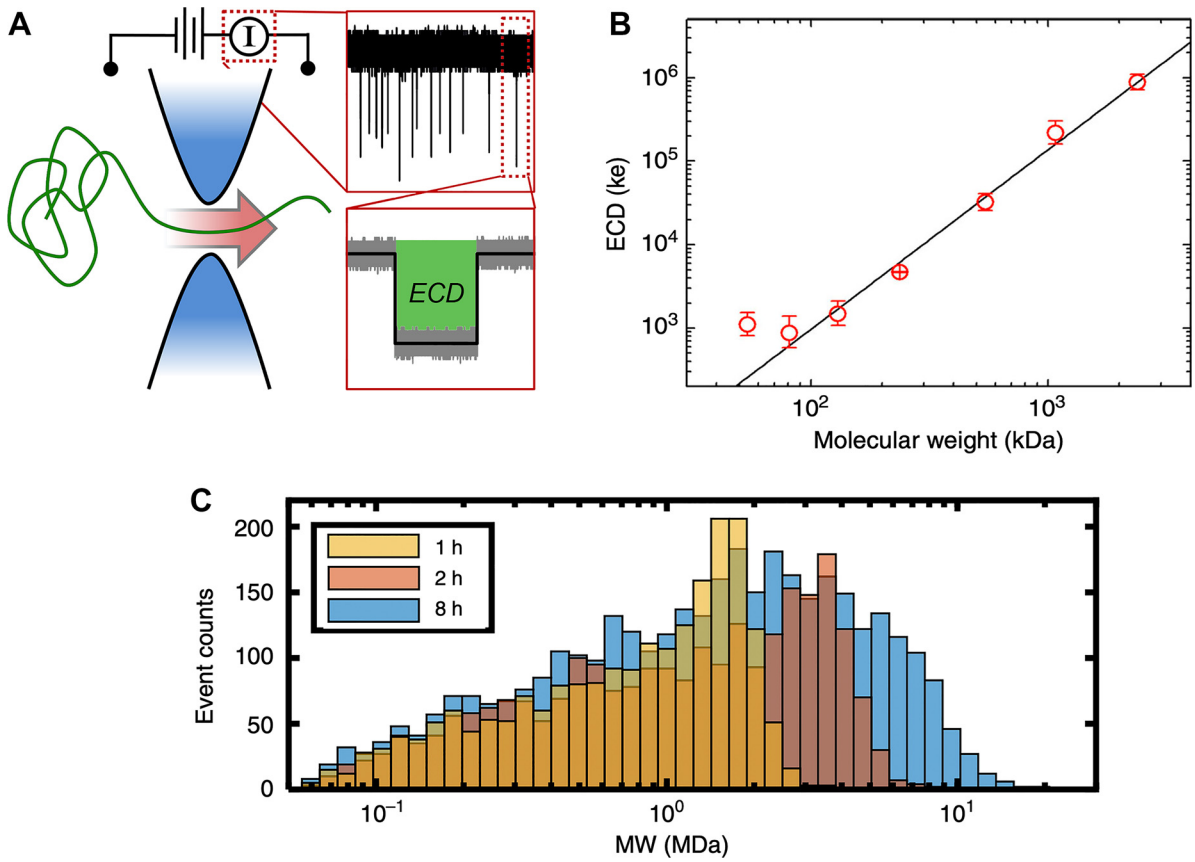

Figure 4. *A*: schematic of the SS-nanopore measurement approach showing a hyaluronan (HA) (green) pulled electrophoretically through a nanometer-scale pore (blue). *Top inset*: example current trace showing molecular translocation signals (spikes). *Bottom inset*: zoom of a translocation signal indicating event charge deficit (ECD) (green). *B*: calibration plot of ECDs for chemoenzymatically synthesized HA standards. Line is a power law fit to the data. Reprinted from Ref. 50 under the Creative Commons CC BY license. *C*: example molecular weight (MW) distribution histograms collected for HA derived from bacterial membrane fragments for indicated times. Reprinted from Ref. 172 under the Creative Commons CC BY license.

porin protein inserted in a suspended lipid membrane, and solid-state (SS-) nanopores (176, 177), composed of single apertures fabricated in a (usually silicon-based) thin-film membrane. Although biological pores have been applied to HA measurement (178), they are generally delicate (due to the lipid membrane) and have yielded limited size capacity. Consequently, our discussion here will focus on their artificial counterparts.

SS-nanopores can be engineered to various dimensions, but HA analysis is typically performed using pores ~7–10 nm in diameter (50). Because the cross-section of a single HA chain is much less than this (<1 nm) (179, 180), molecules are unlikely to translocate linearly, but rather pass in a random, folded conformation that results in complex electrical signatures. To account for this, signal area [called event charge deficit (181), or ECD; see Fig. 4*A*, *bottom inset*] is considered—since folding (higher amplitude) will necessarily be offset by shortened signal duration, this metric is a constant for a given molecular size. Indeed, when quasi-monodisperse HA are analyzed, ECD is found to scale with MW according to a power-law dependency (50), providing a quantitative size calibration (Fig. 4*B*). Consequently, translocation signals can be used to determine HA MW on a molecule-by-molecule basis and a full distribution can be attained by analyzing a representative sampling of HA in a specimen. Commonly, this is achieved through consideration of at least 500 molecules (and more often many thousands), which is measurable in a typical timeframe of 15–20 min from HA samples as small as 10 ng total (50). There is also potential for this sensitivity to be improved further through enhanced extraction or manipulation of experimental variables (e.g., buffer conditions, voltage, etc.).

Notably, the lower MW limit for SS-nanopore measurements is determined by the signal-to-noise ratio (SNR) of the electrical signal. Under common measurement conditions, this enables HA as low as 54 kDa to be resolved readily (50). However, several strategies could be applied to improve this value, including ultra-low noise SS-nanopore devices (182–184) and high bandwidth electrical systems (185, 186). In principle, there is no upper MW limit to the assessment, but extremely large molecules can promote transient clogging of the pore due to entanglement, potentially resulting in an overestimated ECD and thus MW. Nonetheless, measurements of HA up to ~20 MDa have been demonstrated (172).

Understanding the molecular translocation process is critical to ensuring accurate data; for example, if LMW HA is more likely to transit the pore than HMW, the resulting distribution will be biased. In the case of HA, a series of measurements have been performed to determine the relevant dynamics, finding that the rate of translocation signals for a given concentration varies linearly with voltage (50). This is indicative of diffusion-limited translocation (187, 188), such that there is no MW dependence of molecular capture. Consequently, SS-nanopores yield faithful size distributions for arbitrary mixtures of HA; a capacity that has been applied to material from a variety of sources that includes equine synovial fluid (50, 61), human ovarian tissue (62), and HA synthesized in vitro from bacterial membrane fragments (172) (Fig. 4*C*). In addition, the rate of measured translocation signals is known to correlate with HA concentration in solution (50), indicating that SS-nanopores could deliver both MW distribution and quantification in a single measurement if data analysis could compensate for the impact of extraction on the observed concentration.

Conclusions

The myriad physiological roles of HA drives a rising translational interest in the molecule and supports a growing number of use cases that range from structural biomaterial to treatment to diagnostic target. This interest underscores the need for robust analytical approaches to characterize the molecule and as the demand for HA assessment increases, the most appropriate purification strategies and tools will be dictated by the particular needs of the task. For example, in the emerging area of clinical HA diagnostics, evaluation of patient tissues and biofluids will require not only high fidelity and high selectivity extraction processes, but also rapid and sensitive analyses that can provide multidimensional information about the characteristics of physiological HA—especially concentration and polymer size. Of the methodologies surveyed in this review, we believe that SS-nanopore technology may have unique promise for translation given its short measurement time, high sensitivity, broad dynamic range for MW determination, and potential for integrative assessment and automation. However, innovations with other existing technologies continue to be developed as well, suggesting ultimately that improvements in the overall capabilities and availability of HA assessment can be expected. Consequently, it is clear that techniques for probing HA quantity and size will continue to provide new insights into a variety of healthy biological processes and disease pathologies.

GRANTS

The authors acknowledge support from the National Institutes of Health (NIH) Grants R01 GM134226 and P41 EB020594.

DISCLOSURES

No conflicts of interest, financial or otherwise, are declared by the authors.

This article is part of the special collection “Deciphering the Role of Proteoglycans and Glycosaminoglycans in Health and Disease.” Liliana Schaefer, MD, served as Guest Editor of this collection.

AUTHOR CONTRIBUTIONS

M.K.C. and A.R.H. prepared figures; F.R., D.E., I.S., E.R., P.L.D., M.K.C., and A.R.H. drafted manuscript; F.R., D.E., I.S., E.R., P.L.D., M.K.C., and A.R.H. edited and revised manuscript; F.R., D.E., I.S., E.R., P.L.D., M.K.C., and A.R.H. approved final version of manuscript.

REFERENCES

1. **Meyer K**, **Palmer JW.** The polysaccharide of the vitreous humor. *J Biol Chem* 107: 629–634, 1934. doi:10.1016/S0021-9258(18)75338-6.
2. **Gallagher JT**, **Walker A.** Molecular distinctions between heparan-sulfate and heparin—analysis of sulfation patterns indicates that heparan-sulfate and heparin are separate families of N-sulfated polysaccharides. *Biochem J* 230: 665–674, 1985. doi:10.1042/bj2300665.
3. **Sugahara K**, **Mikami T**, **Uyama T**, **Mizuguchi S**, **Nomura K**, **Kitagawa H.** Recent advances in the structural biology of

chondroitin sulfate and dermatan sulfate. *Curr Opin Struct Biol* 13: 612–620, 2003. doi:10.1016/j.sbi.2003.09.011.

4. **Afratis N**, **Gialeli C**, **Nikitovic D**, **Tsegenidis T**, **Karousou E**, **Theocharis AD**, **Pavao MS**, **Tzanakakis GN**, **Karamanos NK.** Glycosaminoglycans: key players in cancer cell biology and treatment. *FEBS J* 279: 1177–1197, 2012. doi:10.1111/j.1742-4658.2012.08529.x.
5. **Broedersz CP**, **MacKintosh FC.** Modeling semiflexible polymer networks. *Rev Mod Phys* 86: 995–1036, 2014. doi:10.1103/RevModPhys.86.995.
6. **Milas M**, **Roure I**, **Berry GC.** Crossover behavior in the viscosity of semiflexible polymers: solutions of sodium hyaluronate as a function of concentration, molecular weight, and temperature. *J Rheol* 40: 1155–1166, 1996. doi:10.1122/1.550778.
7. **Colón E**, **Shytuhina A**, **Cowman MK**, **Band PA**, **Sanggaard KW**, **Enghild JJ**, **Wisniewski H-G.** Transfer of inter-α-inhibitor heavy chains to hyaluronan by surface-linked hyaluronan-TSG-6 complexes. *J Biol Chem* 284: 2320–2331, 2009. doi:10.1074/jbc.M807183200.
8. **Day AJ**, **Prestwich GD.** Hyaluronan-binding proteins: tying up the giant. *J Biol Chem* 277: 4585–4588, 2002. doi:10.1074/jbc.R100036200.
9. **Fraser JR**, **Laurent TC**, **Laurent UB.** Hyaluronan: its nature, distribution, functions and turnover. *J Intern Med* 242: 27–33, 1997. doi:10.1046/j.1365-2796.1997.00170.x.
10. **Cowman MK**, **Lee H-G**, **Schwertfeger KL**, **McCarthy JB**, **Turley EA.** The content and size of hyaluronan in biological fluids and tissues. *Front Immunol* 6: 261, 2015. doi:10.3389/fimmu.2015.00261.
11. **Kendall FE**, **Heidelberger M**, **Dawson MH.** A serologically inactive polysaccharide elaborated by mucoid strains of group A hemolytic Streptococcus. *J Biol Chem* 118: 61–69, 1937. doi:10.1016/S0021-9258(18)74517-1.
12. **Carter GR**, **Annau E.** Isolation of capsular polysaccharides from colonial variants of *Pasteurella multocida*. *Am J Vet Res* 14: 475–478, 1953.
13. **Kang DY**, **Kim W-S**, **Heo IS**, **Park YH**, **Lee S.** Extraction of hyaluronic acid (HA) from rooster comb and characterization using flow field-flow fractionation (FlFFF) coupled with multiangle light scattering (MALS). *J Sep Sci* 33: 3530–3536, 2010. doi:10.1002/jssc.201000478.
14. **Passerotti CC**, **Bonfim A**, **Martins JRM**, **Dall'Oglio MF**, **Sampaio LO**, **Mendes A**, **Ortiz V**, **Srougi M**, **Dietrich CP**, **Nader HB.** Urinary hyaluronan as a marker for the presence of residual transitional cell carcinoma of the urinary bladder. *Eur Urol* 49: 71–75, 2006. doi:10.1016/j.eururo.2005.09.015.
15. **Shirali AC**, **Goldstein DR.** Activation of the innate immune system by the endogenous ligand hyaluronan. *Curr Opin Organ Transplant* 13: 20–25, 2008. doi:10.1097/MOT.0b013e3282f3df04.
16. **Jiang D**, **Liang J**, **Noble PW.** Hyaluronan in tissue injury and repair. *Annu Rev Cell Dev Biol* 23: 435–461, 2007. doi:10.1146/annurev.cellbio.23.090506.123337.
17. **Balazs E.** The physical properties of synovial fluid and the specific role of hyaluronic acid. In: *Disorders of the Knee*, edited by Helfet AJ. Philadelphia: J B Lippincott, 1982, p. 61–74.
18. **Guéchot J**, **Laudat A**, **Loria A**, **Serfaty L**, **Poupon R**, **Giboudeau J.** Diagnostic accuracy of hyaluronan and type III procollagen amino-terminal peptide serum assays as markers of liver fibrosis in chronic viral hepatitis C evaluated by ROC curve analysis. *Clin Chem* 42: 558–563, 1996. doi:10.1093/clinchem/42.4.558.
19. **Neuman MG**, **Cohen LB**, **Nanau RM.** Hyaluronic acid as a non-invasive biomarker of liver fibrosis. *Clin Biochem* 49: 302–315, 2016. doi:10.1016/j.clinbiochem.2015.07.019.
20. **Ono S**, **Imai T**, **Tsumura M**, **Takahashi K**, **Jinnai K**, **Suzuki M**, **Tagawa A**, **Shimizu N.** Increased serum hyaluronic acid in amyotrophic lateral sclerosis: relation to its skin content. *Amyotroph Lateral Scler Mot Neuron Disord* 1: 213–218, 2000. doi:10.1080/14660820050515214.
21. **Back SA**, **Tuohy TMF**, **Chen H**, **Wallingford N**, **Craig A**, **Struve J**, **Luo NL**, **Banine F**, **Liu Y**, **Chang A**, **Trapp BD**, **Bebo BF Jr**, **Rao MS**, **Sherman LS.** Hyaluronan accumulates in demyelinated lesions and inhibits oligodendrocyte progenitor maturation. *Nat Med* 11: 966–972, 2005. doi:10.1038/nm1279.
22. **Akin D**, **Ozmen S**, **Yilmaz ME.** Hyaluronic acid as a new biomarker to differentiate acute kidney injury from chronic kidney disease. *Iran J Kidney Dis* 11: 409–413, 2017.
23. **Petz A**, **Grandoch M**, **Gorski DJ**, **Abrams M**, **Piroth M**, **Schneckmann R**, **Homann S**, **Müller J**, **Hartwig S**, **Lehr S**, **Yamaguchi Y**, **Wight TN**, **Gorressen S**, **Ding Z**, **Kötter S**, **Krüger M**, **Heinen A**, **Kelm M**, **Gödecke A**, **Flögel U**, **Fischer JW.** Cardiac hyaluronan synthesis is critically involved in the cardiac macrophage response and promotes healing after ischemia reperfusion injury. *Circ Res* 124: 1433–1447, 2019. doi:10.1161/CIRCRESAHA.118.313285.
24. **Dahl LB**, **Dahl IM**, **Engström-Laurent A**, **Granath K.** Concentration and molecular weight of sodium hyaluronate in synovial fluid from patients with rheumatoid arthritis and other arthropathies. *Ann Rheum Dis* 44: 817–822, 1985. doi:10.1136/ard.44.12.817.
25. **Band PA**, **Heeter J**, **Wisniewski H-G**, **Liublinska V**, **Pattanayak CW**, **Karia RJ**, **Stabler T**, **Balazs EA**, **Kraus VB.** Hyaluronan molecular weight distribution is associated with the risk of knee osteoarthritis progression. *Osteoarthritis Cartilage* 23: 70–76, 2015. doi:10.1016/j.joca.2014.09.017.
26. **Kraus VB**, **Collins JE**, **Hargrove D**, **Losina E**, **Nevitt M**, **Katz JN**, **Wang SX**, **Sandell LJ**, **Hoffmann SC**, **Hunter DJ**; **OA Biomarkers Consortium.** Predictive validity of biochemical biomarkers in knee osteoarthritis: data from the FNIH OA Biomarkers Consortium. *Ann Rheum Dis* 76: 186–195, 2017. doi:10.1136/annrheumdis-2016-209252.
27. **Lokeshwar VB**, **Öbek C**, **Soloway MS**, **Block NL.** Tumor-associated hyaluronic acid: a new sensitive and specific urine marker for bladder cancer. *Cancer Res* 57: 773–777, 1997.
28. **Thylén A**, **Hjerpe A**, **Martensson G.** Hyaluronan content in pleural fluid as a prognostic factor in patients with malignant pleural mesothelioma. *Cancer* 92: 1224–1230, 2001. doi:10.1002/1097-0142(20010901)92:5<1224::AID-CNCR1441>3.0.CO;2-U.
29. **Franzmann EJ**, **Schroeder GL**, **Goodwin WJ**, **Weed DT**, **Fisher P**, **Lokeshwar VB.** Expression of tumor markers hyaluronic acid and hyaluronidase (HYAL1) in head and neck tumors. *Int J Cancer* 106: 438–445, 2003. doi:10.1002/ijc.11252.
30. **Götte M**, **Yip GW.** Heparanase, hyaluronan, and CD44 in cancers: a breast carcinoma perspective. *Cancer Res* 66: 10233–10237, 2006. doi:10.1158/0008-5472.CAN-06-1464.
31. **Price ZK**, **Lokman NA**, **Ricciardelli C.** Differing roles of hyaluronan molecular weight on cancer cell behavior and chemotherapy resistance. *Cancers (Basel)* 10: 482, 2018. doi:10.3390/cancers10120482.
32. **Mania VM**, **Kallivokas AG**, **Malavaki C**, **Asimakopoulou AP**, **Kanakis J**, **Theocharis AD**, **Klironomos G**, **Gatzounis G**, **Mouzaki A**, **Panagiotopoulos E**, **Karamanos NK.** A comparative biochemical analysis of glycosaminoglycans and proteoglycans in human orthotopic and heterotopic bone. *IUBMB Life* 61: 447–452, 2009. doi:10.1002/iub.167.
33. **Anower-E-Khuda MF**, **Kimata K.** Human blood glycosaminoglycans: isolation and analysis. In: *Glycosaminoglycans*, edited by Balagurunathan K, Nakato H, Desai UR. New York: Springer, 2015, p. 95–103.
34. **Sousa AS**, **Guimarães AP**, **Gonçalves CV**, **Silva IJ**, **Cavalcante CL**, **Azevedo DCS.** Purification and characterization of microbial hyaluronic acid by solvent precipitation and size-exclusion chromatography. *Sep Sci Technol* 44: 906–923, 2009. doi:10.1080/01496390802691281.
35. **Liu Z**, **Zhang F**, **Li L**, **Li G**, **He W**, **Linhardt RJ.** Compositional analysis and structural elucidation of glycosaminoglycans in chicken eggs. *Glycoconj J* 31: 593–602, 2014. doi:10.1007/s10719-014-9557-3.
36. **Nakano T**, **Ikawa N**, **Ozimek L.** Extraction of glycosaminoglycans from chicken eggshell. *Poult Sci* 80: 681–684, 2001. doi:10.1093/ps/80.5.681.
37. **Lago G**, **Oruna L**, **Cremata J**, **Perez C**, **Coto G**, **Lauzan E**, **Kennedy J.** Isolation, purification and characterization of hyaluronan from human umbilical cord residues. *Carbohydr Polym* 62: 321–326, 2005. doi:10.1016/j.carbpol.2005.04.014.
38. **Meyer K**, **Palmer JW.** On glycoproteins. II. The polysaccharides of vitreous humor and of umbilical cord. *J Biol Chem* 114: 689–703, 1936. doi:10.1016/S0021-9258(18)74798-4.
39. **Meyer K**, **Davidson E**, **Linker A**, **Hoffman P.** The acid mucopolysaccharides of connective tissue. *Biochim Biophys Acta* 21: 506–518, 1956. doi:10.1016/0006-3002(56)90188-3.

40. **Watanabe K**, **Oohira A**, **Uramoto I**, **Totsuka T.** Age-related changes in the content and composition of glycosaminoglycans isolated from the mouse skeletal muscle: normal and dystrophic conditions1. *J Biochem* 100: 167–173, 1986. doi:10.1093/oxfordjournals.jbchem.a121689.
41. **Coppa GV**, **Gabrielli O**, **Buzzega D**, **Zampini L**, **Galeazzi T**, **Maccari F**, **Bertino E**, **Volpi N.** Composition and structure elucidation of human milk glycosaminoglycans. *Glycobiology* 21: 295–303, 2011. doi:10.1093/glycob/cwq164.
42. **Margolis RU**, **Margolis RK**, **Chang LB**, **Preti C.** Glycosaminoglycans of brain during development. *Biochemistry* 14: 85–88, 1975. doi:10.1021/bi00672a014.
43. **Svennerholm L**, **Fredman P.** A procedure for the quantitative isolation of brain gangliosides. *Biochim Biophys Acta* 617: 97–109, 1980. doi:10.1016/0005-2760(80)90227-1.
44. **Kilia V**, **Skandalis SS**, **Theocharis AD**, **Theocharis DA**, **Karamanos NK**, **Papageorgakopoulou N.** Glycosaminoglycan in cerebrum, cerebellum and brainstem of young sheep brain with particular reference to compositional and structural variations of chondroitin-dermatan sulfate and hyaluronan. *Biomed Chromatogr* 22: 931–938, 2008. doi:10.1002/bmc.1010.
45. **Barker SA**, **Young NM.** Isolation of hyaluronic acid from human synovial fluid by pronase digestion and gel filtration. *Carbohydr Res* 2: 49–55, 1966. doi:10.1016/S0008-6215(00)81776-0.
46. **Yuan H**, **Amin R**, **Ye X**, **de la Motte CA**, **Cowman MK.** Determination of hyaluronan molecular mass distribution in human breast milk. *Anal Biochem* 474: 78–88, 2015. doi:10.1016/j.ab.2014.12.020.
47. **Ni K**, **Gill A**, **Tseng V**, **Mikosz AM**, **Koike K**, **Beatman EL**, **Xu CY**, **Cao D**, **Gally F**, **Mould KJ**, **Serban KA**, **Schweitzer KS**, **March KL**, **Janssen WJ**, **Nozik-Grayck E**, **Garantziotis S**, **Petrache I.** Rapid clearance of heavy chain-modified hyaluronan during resolving acute lung injury. *Respir Res* 19: 107, 2018. doi:10.1186/s12931-018-0812-1.
48. **Nagy N**, **de la Zerda A**, **Kaber G**, **Johnson PY**, **Hu KH**, **Kratochvil MJ**, **Yadava K**, **Zhao W**, **Cui Y**, **Navarro G**, **Annes JP**, **Wight TN**, **Heilshorn SC**, **Bollyky PL**, **Butte MJ.** Hyaluronan content governs tissue stiffness in pancreatic islet inflammation. *J Biol Chem* 293: 567–578, 2018. doi:10.1074/jbc.RA117.000148.
49. **Tolg C**, **Hamilton SR**, **Zalinska E**, **McCulloch L**, **Amin R**, **Akentieva N**, **Winnik F**, **Savani R**, **Bagli DJ**, **Luyt LG**, **Cowman MK**, **McCarthy JB**, **Turley EA.** A RHAMM mimetic peptide blocks hyaluronan signaling and reduces inflammation and fibrogenesis in excisional skin wounds. *Am J Pathol* 181: 1250–1270, 2012. doi:10.1016/j.ajpath.2012.06.036.
50. **Rivas F**, **Zahid OK**, **Reesink HL**, **Peal BT**, **Nixon AJ**, **DeAngelis PL**, **Skardal A**, **Rahbar E**, **Hall AR.** Label-free analysis of physiological hyaluronan size distribution with a solid-state nanopore sensor. *Nat Commun* 9: 1037, 2018. doi:10.1038/s41467-018-03439-x.
51. **Hill DR**, **Rho HK**, **Kessler SP**, **Amin R**, **Homer CR**, **McDonald C**, **Cowman MK**, **De La Motte CA.** Human milk hyaluronan enhances innate defense of the intestinal epithelium. *J Biol Chem* 288: 29090–29104, 2013. doi:10.1074/jbc.M113.468629.
52. **Osago H**, **Shibata T**, **Hara N**, **Kuwata S**, **Kono M**, **Uchio Y**, **Tsuchiya M.** Quantitative analysis of glycosaminoglycans, chondroitin/dermatan sulfate, hyaluronic acid, heparan sulfate, and keratan sulfate by liquid chromatography–electrospray ionization–tandem mass spectrometry. *Anal Biochem* 467: 62–74, 2014. doi:10.1016/j.ab.2014.08.005.
53. **Lauer ME**, **Mukhopadhyay D**, **Fulop C**, **de la Motte CA**, **Majors AK**, **Hascall VC.** Primary murine airway smooth muscle cells exposed to poly(I,C) or tunicamycin synthesize a leukocyte-adhesive hyaluronan matrix. *J Biol Chem* 284: 5299–5312, 2009. doi:10.1074/jbc.M807965200.
54. **Tolg C**, **Yuan H**, **Flynn SM**, **Basu K**, **Ma J**, **Tse KCK**, **Kowalska B**, **Vulkanesku D**, **Cowman MK**, **McCarthy JB**, **Turley EA.** Hyaluronan modulates growth factor induced mammary gland branching in a size dependent manner. *Matrix Biol* 63: 117–132, 2017. doi:10.1016/j.matbio.2017.02.003.
55. **Tolg C**, **Cowman M**, **Turley E.** Hyaluronan isolation from mouse mammary gland. *Bio-Protoc* 8: e2865, 2018. doi:10.21769/BioProtoc.2865.
56. **Sugitani K**, **Egorova D**, **Mizumoto S**, **Nishio S**, **Yamada S**, **Kitagawa H**, **Oshima K**, **Nadano D**, **Matsuda T**, **Miyata S.** Hyaluronan degradation and release of a hyaluronan-aggrecan complex from perineuronal nets in the aged mouse brain. *Biochim Biophys Acta Gen Subj* 1865: 129804, 2021. doi:10.1016/j.bbagen.2020.129804.
57. **Jandik K**, **Gu K**, **Linhardt R.** Action pattern of polysaccharide lyases on glycosaminoglycans. *Glycobiology* 4: 289–296, 1994. doi:10.1093/glycob/4.3.289.
58. **Margolis RU**, **Margolis RK.** Mucopolysaccharides and glycoproteins. In: *Research Methods in Neurochemistry*, edited by Marks N, Rodnight R. Boston, MA: Springer, 1972, vol. 1, p. 249–284.
59. **Endo M**, **Namiki O**, **Yosizawa Z.** Fractionation with ethanol of human urinary glycosaminoglycans. *Tohoku J Exp Med* 131: 23–28, 1980. doi:10.1620/tjem.131.23.
60. **Hayes AJ**, **Tudor D**, **Nowell MA**, **Caterson B**, **Hughes CE.** Chondroitin sulfate sulfation motifs as putative biomarkers for isolation of articular cartilage progenitor cells. *J Histochem Cytochem* 56: 125–138, 2008. doi:10.1369/jhc.7A7320.20071.
61. **Fasanello DC**, **Su J**, **Deng S**, **Yin R**, **Colville MJ**, **Berenson JM**, **Kelly CM**, **Freer H**, **Rollins A**, **Wagner B**, **Rivas F**, **Hall AR**, **Rahbar E**, **DeAngelis PL**, **Paszek MJ**, **Reesink HL.** Hyaluronic acid synthesis, degradation, and crosslinking in equine osteoarthritis: TNF-α-TSG-6-mediated HC-HA formation. *Arthritis Res Ther* 23: 218, 2021. doi:10.1186/s13075-021-02588-7.
62. **Amargant F**, **Manuel SL**, **Tu Q**, **Parkes WS**, **Rivas F**, **Zhou LT**, **Rowley JE**, **Villanueva CE**, **Hornick JE**, **Shekhawat GS**, **Wei J-J**, **Pavone ME**, **Hall AR**, **Pritchard MT**, **Duncan FE.** Ovarian stiffness increases with age in the mammalian ovary and depends on collagen and hyaluronan matrices. *Aging Cell* 19: e13259, 2020. doi:10.1111/acel.13259.
63. **Itano N**, **Sawai T**, **Yoshida M**, **Lenas P**, **Yamada Y**, **Imagawa M**, **Shinomura T**, **Hamaguchi M**, **Yoshida Y**, **Ohnuki Y**, **Miyauchi S**, **Spicer AP**, **McDonald JA**, **Kimata K.** Three isoforms of mammalian hyaluronan synthases have distinct enzymatic properties. *J Biol Chem* 274: 25085–25092, 1999. doi:10.1074/jbc.274.35.25085.
64. **Itano N**, **Kimata K.** Mammalian hyaluronan synthases. *IUBMB Life* 54: 195–199, 2002. doi:10.1080/15216540214929.
65. **Stern R.** Devising a pathway for hyaluronan catabolism: are we there yet? *Glycobiology* 13: 105R–115R, 2003. doi:10.1093/glycob/cwg112.
66. **Sõoltés L**, **Mendichi R**, **Kogan G**, **Schiller J**, **Stankovská M**, **Arnhold J.** Degradative action of reactive oxygen species on hyaluronan. *Biomacromolecules* 7: 659–668, 2006. doi:10.1021/bm050867v.
67. **Stern R**, **Kogan G**, **Jedrzejas MJ**, **Soltés L.** The many ways to cleave hyaluronan. *Biotechnol Adv* 25: 537–557, 2007. doi:10.1016/j.biotechadv.2007.07.001.
68. **Crawford DHG**, **Murphy TL**, **Ramm LE**, **Fletcher LM**, **Clouston AD**, **Anderson GJ**, **Subramaniam VN**, **Powell LW**, **Ramm GA.** Serum hyaluronic acid with serum ferritin accurately predicts cirrhosis and reduces the need for liver biopsy in C282Y hemochromatosis. *Hepatology* 49: 418–425, 2009. doi:10.1002/hep.22650.
69. **Gudowska M**, **Gruszewska E**, **Panasiuk A**, **Cylwik B**, **Flisiak R**, **S¨widerska M**, **Szmitkowski M**, **Chrostek L.** Hyaluronic acid concentration in liver diseases. *Clin Exp Med* 16: 523–528, 2016. doi:10.1007/s10238-015-0388-8.
70. **Guéchot J**, **Poupon R**, **Poupon R.** Serum hyaluronan as a marker of liver fibrosis. *J Hepatol* 22: 103–106, 1995.
71. **Sasaki E**, **Tsuda E**, **Yamamoto Y**, **Maeda S**, **Inoue R**, **Chiba D**, **Fujita H**, **Takahashi I**, **Umeda T**, **Nakaji S**, **Ishibashi Y.** Serum hyaluronic acid concentration predicts the progression of joint space narrowing in normal knees and established knee osteoarthritis—a five-year prospective cohort study. *Arthritis Res Ther* 17: 283, 2015. doi:10.1186/s13075-015-0793-0.
72. **Saruga T**, **Sasaki E**, **Inoue R**, **Chiba D**, **Ota S**, **Iwasaki H**, **Uesato R**, **Nakaji S**, **Ishibashi Y.** Usefulness of serum hyaluronic acid levels as a predictor of incidence of hand osteoarthritis analyzed by longitudinal analysis from the Iwaki cohort. *Sci Rep* 11: 4074, 2021. doi:10.1038/s41598-021-83693-0.
73. **Delpech B**, **Chevallier B**, **Reinhardt N**, **Julien JP**, **Duval C**, **Maingonnat C**, **Bastit P**, **Asselain B.** Serum hyaluronan (hyaluronic acid) in breast cancer patients. *Int J Cancer* 46: 388–390, 1990. doi:10.1002/ijc.2910460309.
74. **Chen I**, **Dehlendorff C**, **Johansen AZ**, **Jensen BV**, **Krüger MB**, **Pfeiffer P**, **Bjerregaard JK**, **Bojesen SE**, **Nielsen SE**, **Hollander NH**, **Yilmaz M**, **Rasmussen LS**, **Johansen JS.** Prognostic and diagnostic value of serum hyaluronan in patients with pancreatic carcinoma. *J*

Clin Oncol 36: e16249, 2018. doi:10.1200/JCO.2018.36.15_suppl.e16249.

75. **Lokeshwar VB**, **Obek C**, **Pham HT**, **Wei D**, **Young MJ**, **Duncan RC**, **Soloway MS**, **Block NL.** Urinary hyaluronic acid and hyaluronidase: markers for bladder cancer detection and evaluation of grade. *J Urol* 163: 348–356, 2000. doi:10.1016/s0022-5347(05)68050-0.
76. **Morera DS**, **Hennig MS**, **Talukder A**, **Lokeshwar SD**, **Wang J**, **Garcia-Roig M**, **Ortiz N**, **Yates TJ**, **Lopez LE**, **Kallifatidis G**, **Kramer MW**, **Jordan AR**, **Merseburger AS**, **Manoharan M**, **Soloway MS**, **Terris MK**, **Lokeshwar VB.** Hyaluronic acid family in bladder cancer: potential prognostic biomarkers and therapeutic targets. *Br J Cancer* 117: 1507–1517, 2017. doi:10.1038/bjc.2017.318.
77. **Soato M**, **Galesso D**, **Beninatto R**, **Bettella F**, **Guarise C**, **Pavan M.** A versatile and robust analytical method for hyaluronan quantification in crosslinked products and complex matrices. *Carbohydr Res* 503: 108314, 2021. doi:10.1016/j.carres.2021.108314.
78. **Mahoney DJ**, **Aplin RT**, **Calabro A**, **Hascall VC**, **Day AJ.** Novel methods for the preparation and characterization of hyaluronan oligosaccharides of defined length. *Glycobiology* 11: 1025–1033, 2001. doi:10.1093/glycob/11.12.1025.
79. **Volpi N.** On-line HPLC/ESI-MS separation and characterization of hyaluronan oligosaccharides from 2-mers to 40-mers. *Anal Chem* 79: 6390–6397, 2007. doi:10.1021/ac070837d.
80. **Lin W**, **Shuster S**, **Maibach HI**, **Stern R.** Patterns of hyaluronan staining are modified by fixation techniques. *J Histochem Cytochem* 45: 1157–1163, 1997. doi:10.1177/002215549704500813.
81. **de la Motte CA**, **Hascall VC**, **Drazba J**, **Bandyopadhyay SK**, **Strong SA.** Mononuclear leukocytes bind to specific hyaluronan structures on colon mucosal smooth muscle cells treated with polyinosinic acid:polycytidylic acid: inter-α-trypsin inhibitor is crucial to structure and function. *Am J Pathol* 163: 121–133, 2003. doi:10.1016/s0002-9440(10)63636-x.
82. **McDonald B**, **McAvoy EF**, **Lam F**, **Gill V**, **de la Motte C**, **Savani RC**, **Kubes P.** Interaction of CD44 and hyaluronan is the dominant mechanism for neutrophil sequestration in inflamed liver sinusoids. *J Exp Med* 205: 915–927, 2008. doi:10.1084/jem.20071765.
83. **Rilla K**, **Tiihonen R**, **Kultti A**, **Tammi M**, **Tammi R.** Pericellular hyaluronan coat visualized in live cells with a fluorescent probe is scaffolded by plasma membrane protrusions. *J Histochem Cytochem* 56: 901–910, 2008. doi:10.1369/jhc.2008.951665.
84. **Evanko SP**, **Potter-Perigo S**, **Johnson PY**, **Wight TN.** Organization of hyaluronan and versican in the extracellular matrix of human fibroblasts treated with the viral mimetic poly I:C. *J Histochem Cytochem* 57: 1041–1060, 2009. doi:10.1369/jhc.2009.953802.
85. **Twarock S**, **Tammi MI**, **Savani RC**, **Fischer JW.** Hyaluronan stabilizes focal adhesions, filopodia, and the proliferative phenotype in esophageal squamous carcinoma cells. *J Biol Chem* 285: 23276–23284, 2010. doi:10.1074/jbc.M109.093146.
86. **Rowley JE**, **Rubenstein GE**, **Manuel SL**, **Johnson NL**, **Surgnier J**, **Kapitsinou PP**, **Duncan FE**, **Pritchard MT.** Tissue-specific fixation methods are required for optimal in situ visualization of hyaluronan in the ovary, kidney, and liver. *J Histochem Cytochem* 68: 75–91, 2020. doi:10.1369/0022155419884879.
87. **Sõínová R**, **Žádníková P**, **Sõafránková B**, **Nešporová K.** Anti-HA antibody does not detect hyaluronan. *Glycobiology* 31: 520–523, 2021. doi:10.1093/glycob/cwaa118.
88. **Bonnet F**, **Dunham DG**, **Hardingham TE.** Structure and interactions of cartilage proteoglycan binding region and link protein. *Biochem J* 228: 77–85, 1985. doi:10.1042/bj2280077.
89. **Watanabe H**, **Cheung SC**, **Itano N**, **Kimata K**, **Yamada Y.** Identification of hyaluronan-binding domains of aggrecan. *J Biol Chem* 272: 28057–28065, 1997. doi:10.1074/jbc.272.44.28057.
90. **Merrilees MJ**, **Zuo N**, **Evanko SP**, **Day AJ**, **Wight TN.** G1 domain of versican regulates hyaluronan organization and the phenotype of cultured human dermal fibroblasts. *J Histochem Cytochem* 64: 353–363, 2016. doi:10.1369/0022155416643913.
91. **Garcia EA**, **Veridiano AM**, **Martins JRM**, **Nader HB**, **Pinheiro MC**, **Joazeiro PP**, **Toledo OMS.** Hyaluronan involvement in the changes of mouse interpubic tissue during late pregnancy and post-partum. *Cell Biol Int* 32: 913–919, 2008. doi:10.1016/j.cellbi.2008.04.006.
92. **Ling W**, **Regatte RR**, **Navon G**, **Jerschow A.** Assessment of glycosaminoglycan concentration in vivo by chemical exchange-dependent saturation transfer (gagCEST). *Proc Natl Acad Sci USA* 105: 2266–2270, 2008. doi:10.1073/pnas.0707666105.
93. **Engvall E**, **Perlmann P.** Enzyme-linked immunosorbent assay (ELISA) quantitative assay of immunoglobulin-G. *Immunochemistry* 8: 871–874, 1971. doi:10.1016/0019-2791(71)90454-X.
94. **Tengblad A.** Quantitative analysis of hyaluronate in nanogram amounts. *Biochem J* 185: 101–105, 1980. doi:10.1042/bj1850101.
95. **Engström-Laurent A**, **Laurent UBG**, **Lilja K**, **Laurent TC.** Concentration of sodium hyaluronate in serum. *Scand J Clin Lab Invest* 45: 497–504, 1985. doi:10.3109/00365518509155249.
96. **Li X-Q**, **Thonar E-MA**, **Knudson W.** Accumulation of hyaluronate in human lung carcinoma as measured by a new hyaluronate ELISA. *Connect Tissue Res* 19: 243–253, 1989. doi:10.3109/03008208909043899.
97. **Fosang AJ**, **Hey NJ**, **Carney SL**, **Hardingham TE.** An ELISA plate based assay for hyaluronan using biotinylated proteoglycan G1 domain (HA-binding region). *Matrix* 10: 306–313, 1990. doi:10.1016/S0934-8832(11)80186-1.
98. **Martins JRM**, **Passerotti CC**, **Maciel RMB**, **Sampaio LO**, **Dietrich CP**, **Nader HB.** Practical determination of hyaluronan by a new non-competitive fluorescence-based assay on serum of normal and cirrhotic patients. *Anal Biochem* 319: 65–72, 2003. doi:10.1016/S0003-2697(03)00251-3.
99. **Haserodt S**, **Aytekin M**, **Dweik RA.** A comparison of the sensitivity, specificity, and molecular weight accuracy of three different commercially available hyaluronan ELISA-like assays. *Glycobiology* 21: 175–183, 2011. doi:10.1093/glycob/cwq145.
100. **Laurent UB**, **Tengblad A.** Determination of hyaluronate in biological samples by a specific radioassay technique. *Anal Biochem* 109: 386–394, 1980. doi:10.1016/0003-2697(80)90665-x.
101. **Delpech B**, **Bertrand P**, **Maingonnat C.** Immunoenzymoassay of the hyaluronic acid-hyaluronectin interaction: application to the detection of hyaluronic acid in serum of normal subjects and cancer patients. *Anal Biochem* 149: 555–565, 1985. doi:10.1016/0003-2697(85)90613-x.
102. **Goldberg RL.** Enzyme-linked immunosorbent assay for hyaluronate using cartilage proteoglycan and an antibody to keratan sulfate. *Anal Biochem* 174: 448–458, 1988. doi:10.1016/0003-2697(88)90043-7.
103. **West DC**, **Shaw DM**, **Lorenz P**, **Adzick NS**, **Longaker MT.** Fibrotic healing of adult and late gestation fetal wounds correlates with increased hyaluronidase activity and removal of hyaluronan. *Int J Biochem Cell Biol* 29: 201–210, 1997. doi:10.1016/S1357-2725(96)00133-1.
104. **Hartwell SK**, **Srisawang B**, **Kongtawelert P**, **Jakmunee J**, **Grudpan K.** Sequential injection-ELISA based system for online determination of hyaluronan. *Talanta* 66: 521–527, 2005. doi:10.1016/j.talanta.2004.11.032.
105. **Echelon Biosciences**. Hyaluronan Enzyme-Linked Immunosorbent Assay (HA ELISA) (Online). https://www.echelon-inc.com/product/hyaluronan-enzyme-linked-immunosorbent-assay-ha-elisa/ [2022 Jan 7].
106. **Yuan H**, **Tank M**, **Alsofyani A**, **Shah N**, **Talati N**, **LoBello JC**, **Kim JR**, **Oonuki Y**, **de la Motte CA**, **Cowman MK.** Molecular mass dependence of hyaluronan detection by sandwich ELISA-like assay and membrane blotting using biotinylated hyaluronan binding protein. *Glycobiology* 23: 1270–1280, 2013. doi:10.1093/glycob/cwt064.
107. **Ullman EF**, **Kirakossian H**, **Singh S**, **Wu ZP**, **Irvin BR**, **Pease JS**, **Switchenko AC**, **Irvine JD**, **Dafforn A**, **Skold CN.** Luminescent oxygen channeling immunoassay: measurement of particle binding kinetics by chemiluminescence. *Proc Natl Acad Sci USA* 91: 5426–5430, 1994. doi:10.1073/pnas.91.12.5426.
108. **Huang X**, **Schmidt TA**, **Shortt C**, **Arora S**, **Asari A**, **Kirsch T**, **Cowman MK.** A competitive alphascreen assay for detection of hyaluronan. *Glycobiology* 28: 137–147, 2018. doi:10.1093/glycob/cwx109.
109. **Little CB**, **Meeker CT**, **Golub SB**, **Lawlor KE**, **Farmer PJ**, **Smith SM**, **Fosang AJ.** Blocking aggrecanase cleavage in the aggrecan interglobular domain abrogates cartilage erosion and promotes cartilage repair. *J Clin Invest* 117: 1627–1636, 2007 [Erratum in *J Clin Invest* 118: 3812, 2008]. doi:10.1172/JCI30765.
110. **Deed R**, **Rooney P**, **Kumar P**, **Norton JD**, **Smith J**, **Freemont AJ**, **Kumar S.** Early-response gene signalling is induced by angiogenic oligosaccharides of hyaluronan in endothelial cells. Inhibition by non-angiogenic, high-molecular-weight hyaluronan. *Int J Cancer* 71:

251–256, 1997. doi:10.1002/(SICI)1097-0215(19970410)71:2<251::AID-IJC21>3.0.CO;2-J.

111. **Nasreen N**, **Mohammed KA**, **Hardwick J**, **van Horn RD**, **Sanders K**, **Kathuria H**, **Loghmani F**, **Antony VB.** Low molecular weight hyaluronan induces malignant mesothelioma cell (MMC) proliferation and haptotaxis: role of CD44 receptor in MMC proliferation and haptotaxis. *Oncol Res* 13: 71–78, 2002. doi:10.3727/096504002108748105.
112. **Maharjan AS**, **Pilling D**, **Gomer RH.** High and low molecular weight hyaluronic acid differentially regulate human fibrocyte differentiation. *PLoS One* 6: e26078, 2011. doi:10.1371/journal.pone.0026078.
113. **Fuchs K**, **Hippe A**, **Schmaus A**, **Homey B**, **Sleeman JP**, **Orian-Rousseau V.** Opposing effects of high- and low-molecular weight hyaluronan on CXCL12-induced CXCR4 signaling depend on CD44. *Cell Death Dis* 4: e819, 2013. doi:10.1038/cddis.2013.364.
114. **Wu M**, **Du Y**, **Liu Y**, **He Y**, **Yang C**, **Wang W**, **Gao F.** Low molecular weight hyaluronan induces lymphangiogenesis through LYVE-1-mediated signaling pathways. *PLoS One* 9: e92857, 2014. doi:10.1371/journal.pone.0092857.
115. **Gebe JA**, **Yadava K**, **Ruppert SM**, **Marshall P**, **Hill P**, **Falk BA**, **Sweere JM**, **Han H**, **Kaber G**, **Harten IA**, **Medina C**, **Mikecz K**, **Ziegler SF**, **Balaji S**, **Keswani SG**, **Perez Va de J**, **Butte MJ**, **Nadeau K**, **Altemeier WA**, **Fanger N**, **Bollyky PL.** Modified high-molecular-weight hyaluronan promotes allergen-specific immune tolerance. *Am J Respir Cell Mol Biol* 56: 109–120, 2017 [Erratum in *Am J Respir Cell Mol Biol* 57: 259, 2017]. doi:10.1165/rcmb.2016-0111OC.
116. **Mascaró M**, **Pibuel MA**, **Lompardía SL**, **Díaz M**, **Zotta E**, **Bianconi MI**, **Lago N**, **Otero S**, **Jankilevich G**, **Alvarez E**, **Hajos SE.** Low molecular weight hyaluronan induces migration of human choriocarcinoma JEG-3 cells mediated by RHAMM as well as by PI3K and MAPK pathways. *Histochem Cell Biol* 148: 173–187, 2017. doi:10.1007/s00418-017-1559-3.
117. **Kim Y**, **Kessler SP**, **Obery DR**, **Homer CR**, **McDonald C**, **de la Motte CA.** Hyaluronan 35 kDa treatment protects mice from *Citrobacter rodentium* infection and induces epithelial tight junction protein ZO-1 in vivo. *Matrix Biol J Biol* 62: 28–39, 2017. doi:10.1016/j.matbio.2016.11.001.
118. **Petrey AC**, **de la Motte CA.** Hyaluronan, a crucial regulator of inflammation. *Front Immunol* 5: 101, 2014. doi:10.3389/fimmu.2014.00101.
119. **Forrester JV**, **Balazs EA.** Inhibition of phagocytosis by high molecular weight hyaluronate. *Immunology* 40: 435–446, 1980.
120. **Nakamura K**, **Yokohama S**, **Yoneda M**, **Okamoto S**, **Tamaki Y**, **Ito T**, **Okada M**, **Aso K**, **Makino I.** High, but not low, molecular weight hyaluronan prevents T-cell-mediated liver injury by reducing proinflammatory cytokines in mice. *J Gastroenterol* 39: 346–354, 2004. doi:10.1007/s00535-003-1301-x.
121. **Bollyky PL**, **Falk BA**, **Wu RP**, **Buckner JH**, **Wight TN**, **Nepom GT.** Intact extracellular matrix and the maintenance of immune tolerance: high molecular weight hyaluronan promotes persistence of induced CD4 + CD25 + regulatory T cells. *J Leukoc Biol* 86: 567–572, 2009. doi:10.1189/jlb.0109001.
122. **McKee CM**, **Penno MB**, **Cowman M**, **Burdick MD**, **Strieter RM**, **Bao C**, **Noble PW.** Hyaluronan (HA) fragments induce chemokine gene expression in alveolar macrophages. The role of HA size and CD44. *J Clin Invest* 98: 2403–2413, 1996. doi:10.1172/JCI119054.
123. **Taylor KR**, **Yamasaki K**, **Radek KA**, **Di Nardo A**, **Goodarzi H**, **Golenbock D**, **Beutler B**, **Gallo RL.** Recognition of hyaluronan released in sterile injury involves a unique receptor complex dependent on Toll-like receptor 4, CD44, and MD-2. *J Biol Chem* 282: 18265–18275, 2007. doi:10.1074/jbc.M606352200.
124. **Noble PW**, **Lake FR**, **Henson PM**, **Riches DW.** Hyaluronate activation of CD44 induces insulin-like growth factor-1 expression by a tumor necrosis factor-α-dependent mechanism in murine macrophages. *J Clin Invest* 91: 2368–2377, 1993. doi:10.1172/JCI116469.
125. **Horton MR**, **McKee CM**, **Bao C**, **Liao F**, **Farber JM**, **Hodge-DuFour J**, **Puré E**, **Oliver BL**, **Wright TM**, **Noble PW.** Hyaluronan fragments synergize with interferon-gamma to induce the C-X-C chemokines mig and interferon-inducible protein-10 in mouse macrophages. *J Biol Chem* 273: 35088–35094, 1998. doi:10.1074/jbc.273.52.35088.
126. **Horton MR**, **Olman MA**, **Noble PW.** Hyaluronan fragments induce plasminogen activator inhibitor-1 and inhibit urokinase activity in mouse alveolar macrophages: a potential mechanism for impaired fibrinolytic activity in acute lung injury. *Chest* 116: 17S, 1999.
127. **Sugahara KN**, **Murai T**, **Nishinakamura H**, **Kawashima H**, **Saya H**, **Miyasaka M.** Hyaluronan oligosaccharides induce CD44 cleavage and promote cell migration in CD44-expressing tumor cells. *J Biol Chem* 278: 32259–32265, 2003. doi:10.1074/jbc.M300347200.
128. **Fieber C**, **Baumann P**, **Vallon R**, **Termeer C**, **Simon JC**, **Hofmann M**, **Angel P**, **Herrlich P**, **Sleeman JP.** Hyaluronan-oligosaccharide-induced transcription of metalloproteases. *J Cell Sci* 117: 359–367, 2004. doi:10.1242/jcs.00831.
129. **Bourguignon LYW**, **Wong G**, **Earle CA**, **Xia W.** Interaction of low molecular weight hyaluronan (LMW-HA) with CD44 and Toll-like receptors promotes the actin filament-associated protein (AFAP-110)-actin binding and MyD88-NFκB signaling leading to pro-inflammatory cytokine/chemokine production and breast tumor invasion. *Cytoskeleton (Hoboken)* 68: 671–693, 2011. doi:10.1002/cm.20544.
130. **Matou-Nasri S**, **Gaffney J**, **Kumar S**, **Slevin M.** Oligosaccharides of hyaluronan induce angiogenesis through distinct CD44 and RHAMM-mediated signalling pathways involving Cdc2 and gamma-adducin. *Int J Oncol* 35: 761–773, 2009. doi:10.3892/ijo_00000389.
131. **Gao F**, **Liu Y**, **He Y**, **Yang C**, **Wang Y**, **Shi X**, **Wei G.** Hyaluronan oligosaccharides promote excisional wound healing through enhanced angiogenesis. *Matrix Biol J Biol* 29: 107–116, 2010. doi:10.1016/j.matbio.2009.11.002.
132. **Cowman MK**, **Schmidt TA**, **Raghavan P**, **Stecco A.** Viscoelastic properties of hyaluronan in physiological conditions. *F1000Res* 4: 622, 2015. doi:10.12688/f1000research.6885.1.
133. **Hokputsa S**, **Jumel K**, **Alexander C**, **Harding SE.** A comparison of molecular mass determination of hyaluronic acid using SEC/MALLS and sedimentation equilibrium. *Eur Biophys J* 32: 450–456, 2003. doi:10.1007/s00249-003-0299-6.
134. **Moon MH.** Flow field-flow fractionation and multiangle light scattering for ultrahigh molecular weight sodium hyaluronate characterization. *J Sep Sci* 33: 3519–3529, 2010. doi:10.1002/jssc.201000414.
135. **Jing W**, **DeAngelis PL.** Synchronized chemoenzymatic synthesis of monodisperse hyaluronan polymers. *J Biol Chem* 279: 42345–42349, 2004. doi:10.1074/jbc.M402744200.
136. **Jing W**, **Haller FM**, **Almond A**, **DeAngelis PL.** Defined megadalton hyaluronan polymer standards. *Anal Biochem* 355: 183–188, 2006. doi:10.1016/j.ab.2006.06.009.
137. **Kaufman SL**, **Skogen JW**, **Dorman FD**, **Zarrin F**, **Lewis KC.** Macromolecule analysis based on electrophoretic mobility in air: globular proteins. *Anal Chem* 68: 1895–1904, 1996. doi:10.1021/ac951128f.
138. **Kaufman SL.** Analysis of biomolecules using electrospray and nanoparticle methods: the gas-phase electrophoretic mobility molecular analyzer (GEMMA). *J Aerosol Sci* 29: 537–552, 1998. doi:10.1016/S0021-8502(97)00462-X.
139. **Weiss VU**, **Pogan R**, **Zoratto S**, **Bond KM**, **Boulanger P**, **Jarrold MF**, **Lyktey N**, **Pahl D**, **Puffler N**, **Schelhaas M**, **Selivanovitch E**, **Uetrecht C**, **Allmaier G.** Virus-like particle size and molecular weight/mass determination applying gas-phase electrophoresis (native nES GEMMA). *Anal Bioanal Chem* 411: 5951–5962, 2019. doi:10.1007/s00216-019-01998-6.
140. **Malm L**, **Hellman U**, **Larsson G.** Size determination of hyaluronan using a gas-phase electrophoretic mobility molecular analysis. *Glycobiology* 22: 7–11, 2012. doi:10.1093/glycob/cwr096.
141. **Do L**, **Dahl CP**, **Kerje S**, **Hansell P**, **Mörner S**, **Lindqvist U**, **Engström-Laurent A**, **Larsson G**, **Hellman U.** High sensitivity method to estimate distribution of hyaluronan molecular sizes in small biological samples using gas-phase electrophoretic mobility molecular analysis. *Int J Cell Biol* 2015: 938013, 2015. doi:10.1155/2015/938013.
142. **Turner RE**, **Cowman MK.** Cationic dye binding by hyaluronate fragments: dependence on hyaluronate chain length. *Arch Biochem Biophys* 237: 253–260, 1985. doi:10.1016/0003-9861(85)90276-0.
143. **Min H**, **Cowman MK.** Combined alcian blue and silver staining of glycosaminoglycans in polyacrylamide gels: application to electrophoretic analysis of molecular weight distribution. *Anal Biochem* 155: 275–285, 1986. doi:10.1016/0003-2697(86)90437-9.
144. **Lee HG**, **Cowman MK.** An agarose gel electrophoretic method for analysis of hyaluronan molecular weight distribution. *Anal Biochem* 219: 278–287, 1994. doi:10.1006/abio.1994.1267.
145. **Ikegami-Kawai M**, **Takahashi T.** Microanalysis of hyaluronan oligosaccharides by polyacrylamide gel electrophoresis and its

application to assay of hyaluronidase activity. *Anal Biochem* 311: 157–165, 2002. doi:10.1016/s0003-2697(02)00425-6.

146. **Bourguignon LYW**, **Singleton PA**, **Diedrich F**, **Stern R**, **Gilad E.** CD44 interaction with Na+-H+ exchanger (NHE1) creates acidic microenvironments leading to hyaluronidase-2 and cathepsin B activation and breast tumor cell invasion. *J Biol Chem* 279: 26991–27007, 2004. doi:10.1074/jbc.M311838200.
147. **Kooy FK**, **Ma M**, **Beeftink HH**, **Eggink G**, **Tramper J**, **Boeriu CG.** Quantification and characterization of enzymatically produced hyaluronan with fluorophore-assisted carbohydrate electrophoresis. *Anal Biochem* 384: 329–336, 2009. doi:10.1016/j.ab.2008.09.042.
148. **Cowman MK**, **Chen CC**, **Pandya M**, **Yuan H**, **Ramkishun D**, **Lobello J**, **Bhilocha S**, **Russell-Puleri S**, **Skendaj E**, **Mijovic J**, **Jing W.** Improved agarose gel electrophoresis method and molecular mass calculation for high molecular mass hyaluronan. *Anal Biochem* 417: 50–56, 2011. doi:10.1016/j.ab.2011.05.023.
149. **Bhilocha S**, **Amin R**, **Pandya M**, **Yuan H**, **Tank M**, **LoBello J**, **Shytuhina A**, **Wang W**, **Wisniewski H-G**, **de la Motte C**, **Cowman MK.** Agarose and polyacrylamide gel electrophoresis methods for molecular mass analysis of 5- to 500-kDa hyaluronan. *Anal Biochem* 417: 41–49, 2011. doi:10.1016/j.ab.2011.05.026.
150. **Cowman MK.** Methods for hyaluronan molecular mass determination by agarose gel electrophoresis. *Methods Mol Biol* 1952: 91–102, 2019. doi:10.1007/978-1-4939-9133-4_8.
151. **Armstrong SE**, **Bell DR.** Measurement of high-molecular-weight hyaluronan in solid tissue using agarose gel electrophoresis. *Anal Biochem* 308: 255–264, 2002. doi:10.1016/S0003-2697(02)00239-7.
152. **Ruscheinsky M**, **De la Motte C**, **Mahendroo M.** Hyaluronan and its binding proteins during cervical ripening and parturition: dynamic changes in size, distribution and temporal sequence. *Matrix Biol* 27: 487–497, 2008. doi:10.1016/j.matbio.2008.01.010.
153. **Armstrong SE**, **Bell DR.** Relationship between lymph and tissue hyaluronan in skin and skeletal muscle. *Am J Physiol Heart Circ Physiol* 283: H2485–H2494, 2002. doi:10.1152/ajpheart.00385.2002.
154. **Casalino-Matsuda SM**, **Monzon ME**, **Conner GE**, **Salathe M**, **Forteza RM.** Role of hyaluronan and reactive oxygen species in tissue kallikrein-mediated epidermal growth factor receptor activation in human airways. *J Biol Chem* 279: 21606–21616, 2004. doi:10.1074/jbc.M309950200.
155. **Casalino-Matsuda SM**, **Monzón ME**, **Forteza RM.** Epidermal growth factor receptor activation by epidermal growth factor mediates oxidant-induced goblet cell metaplasia in human airway epithelium. *Am J Respir Cell Mol Biol* 34: 581–591, 2006. doi:10.1165/rcmb.2005-0386OC.
156. **Campo GM**, **Avenoso A**, **Campo S**, **D'Ascola A**, **Traina P**, **Samà D**, **Calatroni A.** The antioxidant effect exerted by TGF-1β-stimulated hyaluronan production reduced NF-kB activation and apoptosis in human fibroblasts exposed to FeSo4 plus ascorbate. *Mol Cell Biochem* 311: 167–177, 2008. doi:10.1007/s11010-008-9707-7.
157. **Durigova M**, **Roughley PJ**, **Mort JS.** Mechanism of proteoglycan aggregate degradation in cartilage stimulated with oncostatin M. *Osteoarthritis Cartilage* 16: 98–104, 2008. doi:10.1016/j.joca.2007.05.002.
158. **Duterme C**, **Mertens-Strijthagen J**, **Tammi M**, **Flamion B.** Two novel functions of hyaluronidase-2 (Hyal2) are formation of the glycocalyx and control of CD44-ERM interactions. *J Biol Chem* 284: 33495–33508, 2009. doi:10.1074/jbc.M109.044362.
159. **Campo GM**, **Avenoso A**, **Campo S**, **D'Ascola A**, **Traina P**, **Calatroni A.** Effect of cytokines on hyaluronan synthase activity and response to oxidative stress by fibroblasts. *Br J Biomed Sci* 66: 28–36, 2009. doi:10.1080/09674845.2009.11730241.
160. **Tian X**, **Azpurua J**, **Hine C**, **Vaidya A**, **Myakishev-Rempel M**, **Ablaeva J**, **Mao Z**, **Nevo E**, **Gorbunova V**, **Seluanov A.** High-molecular-mass hyaluronan mediates the cancer resistance of the naked mole rat. *Nature* 499: 346–349, 2013. doi:10.1038/nature12234.
161. **Cowman MK**, **Shortt C**, **Arora S**, **Fu Y**, **Villavieja J**, **Rathore J**, **Huang X**, **Rakshit T**, **Jung GI**, **Kirsch T.** Role of hyaluronan in inflammatory effects on human articular chondrocytes. *Inflammation* 42: 1808–1820, 2019. doi:10.1007/s10753-019-01043-9.
162. **Audam TN**, **Nong Y**, **Tomlin A**, **Jurkovic A**, **Li H**, **Zhu X**, **Long BW**, **Zheng YW**, **Weirick T**, **Brittian KR**, **Riggs DW**, **Gumpert A**, **Uchida S**, **Guo Y**, **Wysoczynski M**, **Jones SP.** Cardiac mesenchymal cells from failing and nonfailing hearts limit ventricular dilation when administered late after infarction. *Am J Physiol Heart Circ Physiol* 319: H109–H122, 2020. doi:10.1152/ajpheart.00114.2020.
163. **Volpi N**, **Maccari F**, **Titze J.** Simultaneous detection of submicrogram quantities of hyaluronic acid and dermatan sulfate on agarose-gel by sequential staining with toluidine blue and Stains-All. *J Chromatogr B Analyt Technol Biomed Life Sci* 820: 131–135, 2005. doi:10.1016/j.jchromb.2005.03.028.
164. **Calabro A**, **Hascall VC**, **Midura RJ.** Adaptation of FACE methodology for microanalysis of total hyaluronan and chondroitin sulfate composition from cartilage. *Glycobiology* 10: 283–293, 2000. doi:10.1093/glycob/10.3.283.
165. **Calabro A**, **Benavides M**, **Tammi M**, **Hascall VC**, **Midura RJ.** Microanalysis of enzyme digests of hyaluronan and chondroitin/dermatan sulfate by fluorophore-assisted carbohydrate electrophoresis (FACE). *Glycobiology* 10: 273–281, 2000. doi:10.1093/glycob/10.3.273.
166. **Calabro A**, **Midura R**, **Wang A**, **West L**, **Plaas A**, **Hascall VC.** Fluorophore-assisted carbohydrate electrophoresis (FACE) of glycosaminoglycans. *Osteoarthritis Cartilage* 9: S16–S22, 2001. doi:10.1053/joca.2001.0439.
167. **Tawada A**, **Masa T**, **Oonuki Y**, **Watanabe A**, **Matsuzaki Y**, **Asari A.** Large-scale preparation, purification, and characterization of hyaluronan oligosaccharides from 4-mers to 52-mers. *Glycobiology* 12: 421–426, 2002. doi:10.1093/glycob/cwf048.
168. **Gao N**, **Lehrman MA.** Alternative sources of reagents and supplies of fluorophore-assisted carbohydrate electrophoresis (FACE). *Glycobiology* 13: 1G–3G, 2003. doi:10.1093/glycob/cwg009.
169. **Seyfried NT**, **Blundell CD**, **Day AJ**, **Almond A.** Preparation and application of biologically active fluorescent hyaluronan oligosaccharides. *Glycobiology* 15: 303–312, 2005. doi:10.1093/glycob/cwi008.
170. **Oonuki Y**, **Yoshida Y**, **Uchiyama Y**, **Asari A.** Application of fluorophore-assisted carbohydrate electrophoresis to analysis of disaccharides and oligosaccharides derived from glycosaminoglycans. *Anal Biochem* 343: 212–222, 2005. doi:10.1016/j.ab.2005.05.039.
171. **Meyer K**, **Rapport MM.** The hydrolysis of chondroitin sulfate by testicular hyaluronidase. *Arch Biochem* 27: 287–293, 1950.
172. **Wei W**, **Faubel JL**, **Selvakumar H**, **Kovari DT**, **Tsao J**, **Rivas F**, **Mohabir AT**, **Krecker M**, **Rahbar E**, **Hall AR**, **Filler MA**, **Washburn JL**, **Weigel PH**, **Curtis JE.** Self-regenerating giant hyaluronan polymer brushes. *Nat Commun* 10: 5527, 2019. doi:10.1038/s41467-019-13440-7.
173. **Ma L**, **Cockroft SL.** Biological nanopores for single-molecule biophysics. *Chembiochem* 11: 25–34, 2010. doi:10.1002/cbic.200900526.
174. **Maglia G**, **Heron AJ**, **Stoddart D**, **Japrung D**, **Bayley H.** Analysis of single nucleic acid molecules with protein nanopores. *Methods Enzymol* 475: 591–623, 2010. doi:10.1016/S0076-6879(10)75022-9.
175. **Ying Y-L**, **Cao C**, **Long Y-T.** Single molecule analysis by biological nanopore sensors. *Analyst* 139: 3826–3835, 2014. doi:10.1039/c4an00706a.
176. **Dekker C.** Solid-state nanopores. *Nat Nanotechnol* 2: 209–215, 2007. doi:10.1038/nnano.2007.27.
177. **Hall AR.** Solid-State nanopores: from fabrication to application. *Microsc Today* 20: 24–29, 2012. doi:10.1017/S1551929512000703.
178. **Fennouri A**, **Przybylski C**, **Pastoriza-Gallego M**, **Bacri L**, **Auvray L**, **Daniel R.** Single molecule detection of glycosaminoglycan hyaluronic acid oligosaccharides and depolymerization enzyme activity using a protein nanopore. *ACS Nano* 6: 9672–9678, 2012. doi:10.1021/nn3031047.
179. **Almond A**, **DeAngelis PL**, **Blundell CD.** Hyaluronan: the local solution conformation determined by NMR and computer modeling is close to a contracted left-handed 4-fold helix. *J Mol Biol* 358: 1256–1269, 2006. doi:10.1016/j.jmb.2006.02.077.
180. **Banerji S**, **Wright AJ**, **Noble M**, **Mahoney DJ**, **Campbell ID**, **Day AJ**, **Jackson DG.** Structures of the Cd44–hyaluronan complex provide insight into a fundamental carbohydrate-protein interaction. *Nat Struct Mol Biol* 14: 234–239, 2007. doi:10.1038/nsmb1201.
181. **Fologea D**, **Gershow M**, **Ledden B**, **McNabb DS**, **Golovchenko JA**, **Li J.** Detecting single stranded DNA with a solid state nanopore. *Nano Lett* 5: 1905–1909, 2005. doi:10.1021/nl051199m.
182. **Steinbock LJ**, **Bulushev RD**, **Krishnan S**, **Raillon C**, **Radenovic A.** DNA translocation through low-noise glass nanopores. *ACS Nano* 7: 11255–11262, 2013. doi:10.1021/nn405029j.

183. **Lee M-H**, **Kumar A**, **Park K-B**, **Cho S-Y**, **Kim H-M**, **Lim M-C**, **Kim Y-R**, **Kim K-B.** A low-noise solid-state nanopore platform based on a highly insulating substrate. *Sci Rep* 4: 7448, 2014. doi:10.1038/srep07448.
184. **Wu R**, **Wang Y**, **Zhu Z**, **Yu C**, **Li H**, **Li B**, **Dong S.** Low-noise solid-state nanopore enhancing direct label-free analysis for small dimensional assemblies induced by specific molecular binding. *ACS Appl Mater Interfaces* 13: 9482–9490, 2021. doi:10.1021/acsami.0c20359.
185. **Rosenstein JK**, **Wanunu M**, **Merchant CA**, **Drndic M**, **Shepard KL.** Integrated nanopore sensing platform with sub-microsecond temporal resolution. *Nat Methods* 9: 487–492, 2012. doi:10.1038/NMETH.1932.
186. **Larkin J**, **Henley RY**, **Muthukumar M**, **Rosenstein JK**, **Wanunu M.** High-bandwidth protein analysis using solid-state nanopores. *Biophys J* 106: 696–704, 2014. .doi:10.1016/j.bpj.2013.12.025.
187. **Wanunu M**, **Morrison W**, **Rabin Y**, **Grosberg AY**, **Meller A.** Electrostatic focusing of unlabelled DNA into nanoscale pores using a salt gradient. *Nat Nanotechnol* 5: 160–165, 2010. doi:10.1038/nnano.2009.379.
188. **Grosberg AY**, **Rabin Y.** DNA capture into a nanopore: interplay of diffusion and electrohydrodynamics. *J Chem Phys* 133: 165102, 2010. doi:10.1063/1.3495481.